Atmos. Chem. Phys., 13, 11259–11276, 2013
www.atmos-chem-phys.net/13/11259/2013/
doi:10.5194/acp-13-11259-2013

Atmospheric Chemistry and Physics Open Access

Impacts of aerosols on the chemistry of atmospheric trace gases: a case study of peroxides and HO_2 radicals

H. Liang[1], Z. M. Chen[1], D. Huang[1], Y. Zhao[1], and Z. Y. Li[1,2]

[1]State Key Laboratory of Environmental Simulation and Pollution Control, College of Environmental Sciences and Engineering, Peking University, Beijing 100871, China
[2]School of Earth and Space Sciences, Peking University, Beijing 100871, China

Correspondence to: Z. M. Chen (zmchen@pku.edu.cn)

Received: 25 April 2013 – Published in Atmos. Chem. Phys. Discuss.: 20 June 2013
Revised: 18 September 2013 – Accepted: 21 October 2013 – Published: 20 November 2013

Abstract. Field measurements of atmospheric peroxides were obtained during the summer on two consecutive years over urban Beijing, which highlighted the impacts of aerosols on the chemistry of peroxide compounds and hydroperoxyl radicals (HO_2). The major peroxides were determined to be hydrogen peroxide (H_2O_2), methyl hydroperoxide (MHP), and peroxyacetic acid (PAA). A negative correlation was found between H_2O_2 and PAA in rainwater, providing evidence for a conversion between H_2O_2 and PAA in the aqueous phase. A standard gas phase chemistry model based on the NCAR Master Mechanism provided a good reproduction of the observed H_2O_2 profile on non-haze days but greatly overpredicted the H_2O_2 level on haze days. We attribute this overprediction to the reactive uptake of HO_2 by the aerosols, since there was greatly enhanced aerosol loading and aerosol liquid water content on haze days. The discrepancy between the observed and modeled H_2O_2 can be diminished by adding to the model a newly proposed transition metal ion catalytic mechanism of HO_2 in aqueous aerosols. This confirms the importance of the aerosol uptake of HO_2 and the subsequent aqueous phase reactions in the reduction of H_2O_2. The closure of HO_2 and H_2O_2 between the gas and aerosol phases suggests that the aerosols do not have a net reactive uptake of H_2O_2, because the conversion of HO_2 to H_2O_2 on aerosols compensates for the H_2O_2 loss. Laboratory studies for the aerosol uptake of H_2O_2 in the presence of HO_2 are urgently required to better understand the aerosol uptake of H_2O_2 in the real atmosphere.

1 Introduction

Peroxides play important roles in atmospheric chemical processes. They serve as oxidants both in their own right and as a reservoir species for HO_x (OH and HO_2) radicals, the principle oxidants in the troposphere (Lee et al., 2000; Reeves and Penkett, 2003). Among the peroxides, hydrogen peroxide (H_2O_2), methyl hydroperoxide (MHP, CH_3OOH), and peroxyacetic acid (PAA, $CH_3C(O)OOH$) are of the most concern. It is well known that H_2O_2, together with organic peroxides including MHP and PAA, can oxidize the dissolved S(IV) to S(VI). This results in the formation of sulfate aerosols in the atmospheric aqueous phase, particularly under low pH conditions (Penkett et al., 1979; Calvert et al., 1985; Lind et al., 1987; Gaffney et al., 1987), and contributes to the formation of up to 60 % of the sulfate aerosols in the global atmosphere (Feichter et al., 1996). It has also been suggested that H_2O_2 performs an important function in the formation of secondary organic aerosols (SOA) in the isoprene oxidation system (Claeys et al., 2004; Böge et al., 2006). MHP has been recognized as the most abundant organic peroxide over the past years, with a level similar to H_2O_2 (e.g., Frey et al., 2005; X. Zhang et al., 2012). The feature of MHP that is of most concern is its correlation with formaldehyde (HCHO). The combination of the methyl peroxy radical (CH_3O_2) and the HO_2 radical will yield either MHP (R1) or HCHO (R2) as it undergoes different reaction channels. In addition, CH_3O_2 can react with NO to yield HCHO (Reactions R3–R4) in high NO_x regions.

$$CH_3O_2 + HO_2 \rightarrow CH_3OOH + O_2 \quad (R1)$$

$$CH_3O_2 + HO_2 \rightarrow HCHO + H_2O + O_2 \quad (R2)$$

$$CH_3O_2 + NO \rightarrow CH_3O + NO_2 \quad (R3)$$

$$CH_3O + O_2 \rightarrow HCHO + HO_2 \quad (R4)$$

HCHO is also a reservoir species for HO_x radicals, and its photochemical frequency is an order of magnitude higher than that for MHP (Sander et al., 2011). Therefore, the competitive generation of MHP and HCHO will sequentially determine the production of HO_x radicals. Moreover, MHP has a longer lifetime than H_2O_2 and therefore is more readily transported at large scales, leading to a redistribution of radicals (Cohan et al., 1999). PAA has received more attention in the past few years, mainly due to its correlation with peroxyacetic nitrate (PAN, $CH_3C(O)OONO_2$) (Zhang et al., 2010; Phillips et al., 2013). Like MHP, PAA is also a product of competitive reactions. PAA is produced when the acetyl peroxy radical, $CH_3C(O)O_2$, reacts with HO_2 (Reaction R5); whereas PAN forms when $CH_3C(O)O_2$ combines with NO_2 (Reaction R6). Reactions (R5) and (R6) have a similar reaction rate constant; therefore, PAN is more readily generated under high NO_x conditions. Because PAN can rapidly decompose back to $CH_3C(O)O_2$ due to its thermal instability (Reaction R7), the thermally stable PAA can serve as an important sink for $CH_3C(O)O_2$ in warm conditions (Phillips et al., 2013).

$$CH_3C(O)O_2 + HO_2 \rightarrow CH_3C(O)OOH + O_2 \quad (R5)$$

$$CH_3C(O)O_2 + NO_2 \rightarrow CH_3C(O)OONO_2 \quad (R6)$$

$$CH_3C(O)OONO_2 \rightarrow CH_3C(O)O_2 + NO_2 \quad (R7)$$

Furthermore, PAA has been determined at a level approaching or even exceeding that of H_2O_2 and MHP (Zhang et al., 2010; Phillips et al., 2013). Stein and Saylor (2012) suggest that the PAA-initiated oxidation is important for the conversion of S(IV) to sulfate in the atmospheric aqueous phase under certain conditions.

Aerosols are ubiquitous in the atmosphere and play an important role in atmospheric physical and chemical processes. The abundance and state of the aerosols affect the fate and behavior of trace gases. These impacts are generally placed into two categories: (i) aerosols affect the flux of solar radiation and hence the photochemical activities of traces gases (e.g., R. V. Martin et al., 2003; Li et al., 2011); and (ii) aerosols provide sites for heterogeneous reactions of trace gases. Peroxides are directly or indirectly involved in both of these impacts. Aerosols will decrease the HO_2 radicals, which are a photochemical product as well as a precursor of peroxides, by taking up HO_2 radicals and attenuating solar radiation. A number of laboratory studies revealed that the aerosols have great capacity to take up HO_2 radicals, although the reported values have considerable discrepancy, ranging from < 0.01 to 0.40, depending on the components of the particles and experimental conditions (e.g., Bedjanian et al., 2005, 2013; Thornton and Abbatt, 2005; Taketani et al., 2008, 2009, 2010, 2012; George et al., 2013). Laboratory studies have also suggested that the reactive uptake of HO_2 on aerosols will potentially lead to the production of H_2O_2 (Loukhovitskaya et al., 2009); joint field observations of HO_2 and H_2O_2, however, suggested that the HO_2 uptake will not lead to an increase in gaseous H_2O_2 (Wang et al., 2003; Cantrell et al., 2003; Mao et al., 2010). Obviously, more pertinent laboratory and field studies are needed to resolve this contradiction. Aerosols also have a direct effect on peroxides. The attenuation of solar radiation by aerosols will lead to the reduced photolysis of peroxides. Aerosols will take up H_2O_2, resulting in a decrease of gaseous H_2O_2; this has been demonstrated by laboratory studies (Pradhan et al., 2010a, b; Zhao et al., 2011, 2013), modelings (de Reus et al., 2005), and observations (He et al., 2010). In summary, aerosols affect both the formation and removal of peroxides and sequentially influence the atmospheric oxidation capacity and the budget of HO_x radicals; however, the exact kinetic parameters and mechanisms have remained very uncertain to date.

Haze is a result of intensive aerosol pollution. Haze can significantly strengthen the effects of aerosols, leading to a narrowing of atmospheric visibility, a critical reduction in solar radiation flux, and substantial negative impacts on public health (e.g., Chameides et al., 1999; Yadav et al., 2003; Sun et al., 2006; Hyslop, 2009). Beijing, China, a megacity with a population of 20 million, experiences frequent haze due to its high levels of particulate matter pollution. For example, in January 2013, Beijing endured a lengthy dense haze episode and had only five non-haze days in the whole month (Ma et al., 2013). Although many recent studies have focused on atmospheric components in both the gas and aerosol phases during haze episodes (Sun et al., 2006; Wang et al., 2006; Yu et al., 2011; Duan et al., 2012; Guo et al., 2012), the cycling and budget of oxidants in the hazy atmosphere over Beijing remain poorly understood. Since 2006, we have measured atmospheric peroxides in Beijing during the summertime (He et al., 2010; Zhang et al., 2010; X. Zhang, 2012), with the goal of understanding the atmospheric oxidation capacity and chemical reaction mechanisms of trace gases in

this area. Fortunately, we find that field measurement data in August 2010 and August 2011 are appropriate for studying the impacts of aerosols on peroxides. The observational days were relatively clear and sunny in August 2010, and a haze episode occurred in August 2011. The meteorological conditions during these two periods were similar and the emissions of primary trace gases were presumed to vary little due to their stable sources. Thus, the data from these two years are highly comparable. In this study, we compared the levels of peroxides and other trace gases on non-haze and haze days, and then we used a box model to investigate how aerosols affected the budgets of H_2O_2 and HO_2.

2 Experimental section

2.1 Measurement site description

Atmospheric peroxide observations were conducted during the summers of 2010 and 2011 on the campus of Peking University (PKU, 39.991° N, 116.304° E), situated northwest of urban Beijing, the capital city of China. A series of observations for peroxides have been performed at this site since 2006 (He et al., 2010; Zhang et al., 2010, X. Zhang, 2012). East and north of the campus are two major traffic thoroughfares where traffic jams occur frequently. The observatory was set up on the top of a six-story building with the sampling inlet at ∼ 26 m above the ground. In addition to peroxide measurements, other trace gases (CO, SO_2, NO, NO_2, O_3, etc.), meteorological parameters (temperature, relative humidity, wind direction, and wind speed), and aerosols were measured at the same time. During August 2010, the mean temperature was 28.9 ± 3.6 °C (mean ± standard variation, the same hereafter), the mean relative humidity (RH) was 59.4 ± 19.6 %, the mean wind speed was 2.0 ± 1.2 m s^{-1}, and the mean wind direction was $230.6 \pm 67.5°$. During August 2011, the mean temperature was 28.2 ± 3.6 °C, the mean RH was 68.6 ± 14.6 %, the mean wind speed was 1.5 ± 0.9 m s^{-1}, and the mean wind direction was $226.3 \pm 85.0°$.

2.2 Sampling and analyzing method for peroxides

The instrument for taking peroxide measurements was placed in a room on the top floor, where several air conditioners were assembled to stabilize the temperature to around 28 °C. The sampling inlet was mounted on the roof where it could collect intensively mixed air samples. Air was drawn into a scrubbing coil by a vacuum pump through ∼ 6 m of Teflon tubing (1/4 inch outside diameter) with a flow rate of 2.7 slm (standard liters per minute); thus, the residence time was no more than 2 s in the tubing. The scrubbing coil was a glass-made collector at a controlled temperature of 4 °C. The eluent, 5×10^{-3} M phosphoric acid (H_3PO_4, pH = 3.5), was pumped into the scrubbing coil at a rate of 0.2 mL min^{-1} to dissolve the sampled air. The collection efficiencies of the scrubbing coil were determined to be ∼ 100 % for H_2O_2 and ∼ 85 % for MHP in our previous work (Hua et al., 2008), and we assumed them to be ∼ 85 % for PAA in the present study since the Henry's law constant for PAA is on the same order as that for MHP.

Once collected, the air samples dissolved in the eluent were injected automatically into the HPLC system by an auto sampler for analysis. We pumped 5×10^{-3} M H_3PO_4 (pH = 3.5) into the column as a mobile phase at a flow rate of 0.5 mL min^{-1} using an HPLC pump (Agilent 1100). After separation in the column, the peroxide components in the air samples were mixed with p-hydroxyphenylacetic acid (PHPAA) in the presence of hemin catalyst, and reacted to form a stable fluorescent dimer for fluorescence detection using a fluorescence detector (Agilent 1200). During rainfalls, rain samples were collected into vials using a glass funnel and immediately injected into the HPLC system for analysis.

The ambient relative humidity can affect the flow rate of the eluent and hence the calculation of the peroxide concentration; therefore, it is necessary to calibrate the flow rate. The volume of water flowing through the scrubbing coil per minute that is brought in with the sampled air can be calculated as

$$V_1 = \frac{\mathrm{RH}\, p_{\mathrm{H_2O}}\, V\, M_{\mathrm{H_2O}}}{R\, T\, \rho_{\mathrm{H_2O}}} \quad (1)$$

where RH is the ambient relative humidity, $p_{\mathrm{H_2O}}$ is the saturated vapor pressure of water, V is the air flow rate driven by the vacuum pump, $M_{\mathrm{H_2O}}$ is the molecular weight of water, R is the universal gas constant (8.314 J mol^{-1} K^{-1}), T is the temperature of the sampled air, and $\rho_{\mathrm{H_2O}}$ is the density of liquid water (1 g mL^{-1} at 4 °C).

Similarly, the water volume exiting the scrubbing coil can be given as

$$V_2 = \frac{100\% \times 813.27\mathrm{Pa} \times 2.7\ \mathrm{L\ min^{-1}} \times 18\mathrm{g\ mol^{-1}}}{8.314\ \mathrm{J\ mol^{-1}K^{-1}} \times 1\ \mathrm{g\ mL^{-1}} \times 277.15\mathrm{K}} = 0.017\mathrm{mL\ min^{-1}}. \quad (2)$$

The above equation is based on the assumption that the air leaving the scrubbing coil is at a temperature of 4 °C and is water saturated. The flow rate of the eluent should then be corrected to the following:

$$\begin{aligned}\text{Flow rate} &= 0.200\ \mathrm{mL\ min^{-1}} + V_1 - V_2 \\ &= 0.183\ \mathrm{mL\ min^{-1}} + V_1.\end{aligned} \quad (3)$$

After this calibration, the change in H_2O_2 concentrations is less than 10 %.

Our method has been carefully evaluated in the literature (e.g. Sauer et al., 1996, 2001) and in our previous study (Hua et al., 2008). The heterogeneous decomposition and

the artifact production of peroxides in the tubing were negligible. The multipoint calibration showed that the peroxide presented a good linear response in a wide concentration range relative to the atmosphere. In the field, single point calibrations were done twice a day with a mixing standard solution. The largest uncertainty came from the interference of SO_2. H_2O_2 concentrations were underestimated by $\sim 10\,\%$, $\sim 30\,\%$ and $\sim 50\,\%$ when SO_2 concentrations were 10, 25, 50 ppbv (parts per billion by volume), respectively. The average concentrations of SO_2 were determined to be 4.0 ± 2.6 ppbv in August 2010 and 2.1 ± 1.7 ppbv in August 2011, indicating that the H_2O_2 loss caused by SO_2 interference was typically less than 10 % during our measurements. The loss of organic peroxides caused by SO_2 interference was smaller than that of H_2O_2. Therefore, our observational data for the peroxides were reliable. Further details on this method can be found in Hua et al. (2008).

2.3 Measurement method for other trace gases and meteorological parameters

The trace gases were monitored using a series of specialized continuous online analyzers (Thermo 48i, 43i, 42i, and 49i analyzers for CO, SO_2, NO-NO_2-NO_x, and O_3, respectively). The mass concentration of $PM_{2.5}$ was determined by TEOM 1400A analyzer. The time resolution for all of these species was 1 min. Meteorological parameters including temperature, RH, wind speed, and wind direction were recorded continuously by a weather station (Met One Instruments Inc., USA).

2.4 Method for model calculation

2.4.1 Description of the basic model

The model used in the present study is a photochemical box model based on the NCAR Master Mechanism (Madronich and Calvert, 1990; version 2.4.03; hereafter NCAR_MM). The mechanism contains nearly 2000 species and 5000 gas phase reactions. The reaction rates for the major reactions are in agreement with those recommended in Sander et al. (2011).

The box model does not take into account transport and dilution processes, but it includes the variation in the height of the planetary boundary layer (PBL). Deposition is also included and its rate varies with the PBL height. In the box model, most input parameters could be time related. A tropospheric ultraviolet and visible (TUV) radiation model is coupled online to calculate the photolysis rate. In this study, the box model is applied to study the atmospheric fate of H_2O_2 under different conditions.

2.4.2 Model extension

The box model is extended with aqueous phase reactions regarding the chemistry of HO_x and H_2O_2. The aqueous phase reactions are chiefly drawn from a chemical aqueous phase radical mechanism (CAPRAM 2.4; Ervens et al., 2003) and Mao et al. (2013) (See Table S1). The uptake and volatilization of trace gases are described by the resistance model (Schwartz, 1986) as first-order reactions, with rate constants as follows:

$$k_{\mathrm{in}} = \left(\frac{r}{D_{\mathrm{g}}} + \frac{4}{\omega \alpha} \right)^{-1} A_{\mathrm{s}} \tag{4}$$

and

$$k_{\mathrm{out}} = k_{\mathrm{in}} \frac{1000}{\mathrm{LWC} K_{\mathrm{H}} RT}. \tag{5}$$

In these equations, r is the surface area-weighted radius of particles (m), D_{g} is the gas phase diffusion coefficient ($\mathrm{m^2\,s^{-1}}$), α is the mass accommodation coefficient assumed to be unity in the present study, A_{S} is the aerosol surface area available for the phase transfer ($\mathrm{m^2\,m^{-3}}$), LWC is the liquid water content (fixed to $\mathrm{m^3\,m^{-3}}$), K_{H} is the physical Henry's law constant ($\mathrm{M\,atm^{-1}}$), R is the universal gas constant ($8.206 \times 10^{-2}\,\mathrm{atm\,M^{-1}\,K^{-1}}$), T is the ambient temperature (K), and ω is the mean molecular speed ($\mathrm{m\,s^{-1}}$) given by

$$\omega = \sqrt{\frac{8RT}{\pi M}}, \tag{6}$$

where M is the molecular weight of the trace gases ($\mathrm{kg\,mol^{-1}}$). SO_2, O_2, O_3, and H_2O_2 are assumed to be intensively mixed in the aqueous aerosols due to their long lifetime in the aqueous phase. Since aqueous HO_2 has a short lifetime, the surface concentration of HO_2 is different from its bulk concentration and is corrected according to Mao et al. (2013) (see the Supplement). The aqueous OH concentration is calculated on the basis of the aqueous phase steady state since the uptake of OH from the gas phase is unimportant.

3 Results and discussion

3.1 Peroxides in general

Measurements were performed in August 2010 and August 2011. The predominant peroxides in the gas phase were determined to be H_2O_2, MHP, and PAA. Considering the availability by date of supporting data for meteorological parameters, trace gases, and aerosols, we focus our analysis and discussion on observational data from 7–15 August 2010 and 10–18 August 2011. The time series and averaged diurnal variations of peroxides on those dates are illustrated in Figs. 1 and 2, and the statistical data are summarized in Table 1. It

Table 1. Summary of atmospheric peroxide concentrations (ppbv) in August 2010 and August 2011, urban Beijing.

		August 2010			August 2011		
		H_2O_2	MHP	PAA	H_2O_2	MHP	PAA
	D.L.[a]	0.008	0.120	0.013	0.009	0.090	0.012
24 h	N	503	503	503	654	654	654
	mean (±S.D.[b])	0.20(±0.28)	0.25(±0.12)	0.19(±0.16)	0.10(±0.22)	0.26(±0.17)	0.21(±0.34)
	median	0.08	0.23	0.13	0.01	0.22	0.08
	maximum	1.59	1.13	0.75	2.08	1.10	2.00
Daytime (08:00–20:00 LT[c])	N	248	248	248	322	322	322
	mean (±S.D.)	0.24(±0.29)	0.25(±0.10)	0.23(±0.18)	0.11(±0.23)	0.25(±0.15)	0.30(±0.42)
	median	0.11	0.23	0.18	0.01	0.22	0.09
	maximum	1.33	1.13	0.73	1.56	1.10	2.00
Nighttime (20:00–08:00 LT)	N	254	254	254	332	332	332
	mean (±S.D.)	0.17(±0.27)	0.25(±0.11)	0.16(±0.14)	0.09(±0.21)	0.27(±0.18)	0.14(±0.21)
	median	0.05	0.23	0.10	0.01	0.23	0.07
	maximum	1.59	0.72	0.75	2.08	0.97	1.07

[a]D.L.: detection limit, [b]S.D.: standard deviation, [c]LT: local time.

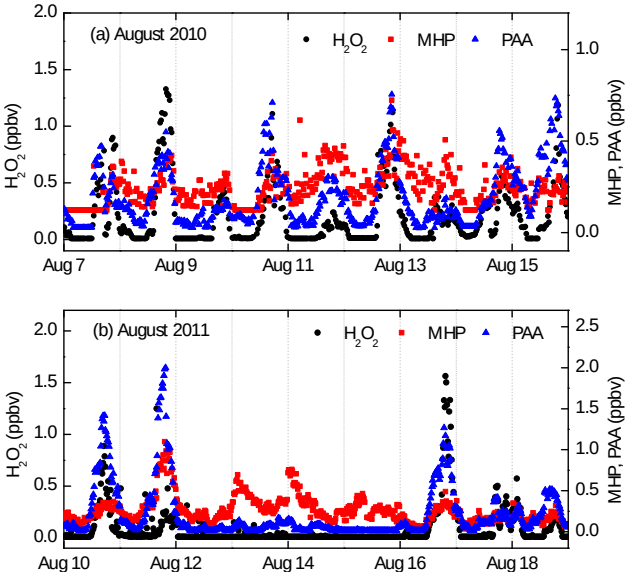

Fig. 1. Temporal profiles for peroxides in the summers of 2010 and 2011.

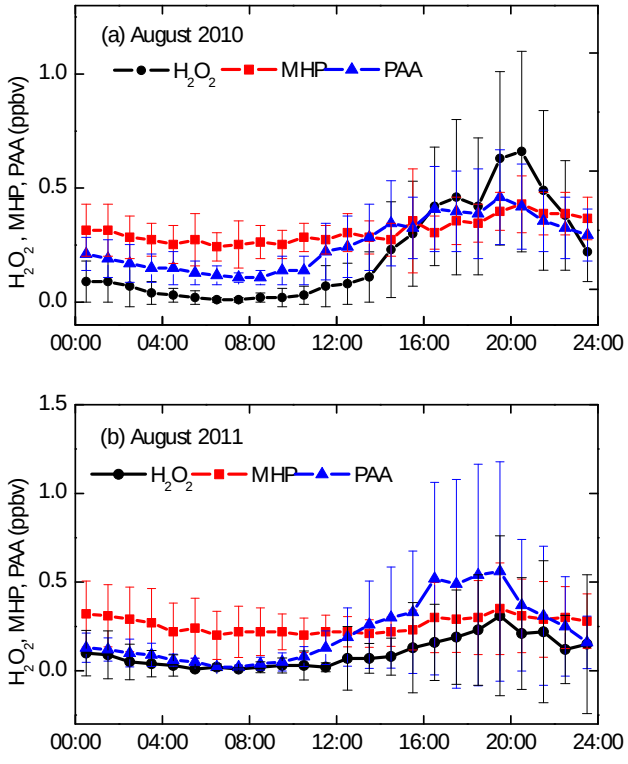

Fig. 2. Hourly-averaged diurnal cycles for peroxides in the summer of 2010 and 2011.

should be noted that the value below the instrument detection limit was treated as equal to the value of detection limit.

The observed peroxides for these two summers over Beijing showed three different points compared to previous observations. First, organic peroxides accounted for a large proportion of the total peroxides. MHP and PAA together composed 80 % of the concentration of total observed peroxides (i.e., H_2O_2+ MHP + PAA); this was much greater than that observed in other sites (summarized in, e.g., Lee et al., 2000; Walker et al., 2006; Kim et al., 2007; Hua et al., 2008). Noticeably, PAA was often observed having a high level of ∼ 1 ppbv. Combining the results of the peroxides observed in 2006, 2007, and 2008 (He et al., 2010; Zhang et al., 2010), we conclude that PAA is a major component of the organic peroxides over Beijing in the summer. Very recently, Phillips et al. (2013) measured PAA in a boreal forest in Finland during the summer using iodide chemical ionization mass spectrometry and found a maximum concentration of 1.2 ppbv, close to the value in our observations.

These studies reveal that PAA may play an important role in atmospheric chemistry. Second, the diurnal maxima shifted toward the evening. In the summer in Beijing, interestingly, the diurnal maxima of peroxides seems to have shifted from 15:00–19:00 local time (LT) in 2006–2008 (He et al., 2010; Zhang et al., 2010) to 17:00–21:00 LT in 2010–2011 (the present study). This delay is possibly caused by the enhanced NO_x, which is associated with an increasing vehicle population. Fleming et al. (2006) found that high NO_x in daytime would lead to a suppression of the peroxy radical level via the repartitioning of peroxy radicals to alkoxy radicals. This subsequently leads to a shift of the peroxy radical time profile toward the evening. As a consequence, the peak of the peroxides would also shift toward the evening since these peroxy radicals are precursors for peroxides. Third, the removal rates of peroxides are fast, particularly at night. The nighttime removal rates of peroxides were estimated with concentration-to-time slopes between 20:30 and 05:30 in the hourly average diurnal profile in August 2010, as shown in Fig. 2a. During this period, the formation of peroxides was weak and thus could be neglected. The average removal rates are calculated to be $1.1 \times 10^{-4}\,s^{-1}$ for H_2O_2, $1.7 \times 10^{-5}\,s^{-1}$ for MHP, and $4.8 \times 10^{-5}\,s^{-1}$ for PAA. To our knowledge, dry deposition dominates the removal of peroxides at night. Considering the nighttime PBL height of ~ 500 m (Sun et al., 2012) in summertime Beijing, we require an average dry deposition velocity of $5.5\,cm\,s^{-1}$ for H_2O_2, $0.85\,cm\,s^{-1}$ for MHP, and $2.4\,cm\,s^{-1}$ for PAA in order to explain the corresponding removal rates of peroxides. The dry deposition velocities for peroxides, however, have been reported over a wide range. For H_2O_2, they range from 0.1 to $5.0\,cm\,s^{-1}$ (Table 2), depending on differences in the underlying surface. The higher values were usually observed (or modeled) over the forest, where the surface resistance is typically smaller. The values in other regions are much lower. Therefore, the dry deposition velocity of H_2O_2 over urban Beijing should be much lower than $5.5\,cm\,s^{-1}$, which is the level needed to explain the nighttime removal of H_2O_2 deposition. MHP and PAA have a much lower dry deposition velocity, 30 times slower than H_2O_2, due to their low solubility (Hauglustaine et al., 1994). In summary, we propose that dry deposition only accounts for part of the nighttime removal of peroxides over Beijing. Apparently, photochemical removal pathways, including OH-initiated reaction and photolysis, are unimportant at night. Therefore, heterogeneous reactions may play a potentially important role in the removal of peroxides.

It is found that the hourly averaged diurnal profiles for H_2O_2, MHP, and PAA are similar, as illustrated in Fig. 2. The peroxides rose rapidly during the day when the solar radiation was strong, implying that the local photochemistry contributed dominantly to these peroxides. According to the removal rates of peroxides mentioned previously, the atmospheric lifetimes of these species are only on the order of several hours, implying that regional transport is unlikely to be important as their source. The transport of other trace gases, however, may affect the generation of peroxides. To understand the impacts of air masses, we used the NOAA Hysplit (hybrid single-particle lagrangian integrated trajectory) model (Draxler and Rolph, 2012; http://ready.arl.noaa.gov/HYSPLIT.php) to plot 48 h backward trajectories of air masses for the observed periods. The trajectories are determined a four-hour interval. It turns out that the dominant air masses over our observation site can be divided into two categories: continental (northwesterly and southwesterly) and marine (southeasterly) originated air masses. Figure 3 compares the observed peroxides in the continental and marine air masses. It can be seen that MHP tends to be slightly higher in the marine sector, while H_2O_2 and PAA are higher in the continental sector. The high MHP level in the marine air mass was also reported in several previous observations (Klippel et al., 2011; X. Zhang et al., 2012) and was explained by the emissions of methane (CH_4) and methyl iodide (CH_3I) from the ocean. These methyl compounds serve as precursors for the photochemical formation of MHP. The atmospheric lifetime was reported as 4–8 d for CH_3I (Hu et al., 2012) and 9.1 yr for CH_4 (Prather et al., 2012). Due to their long lifetimes, these precursors of MHP could be transported with the air mass. On the other hand, the moisture accompanying the marine air masses would lead to high humidity and liquid water content, which would strengthen the removal of peroxides.

3.2 Rainwater peroxides and aqueous phase conversion

On 24 July 2011 the rainfall started at $\sim$ 14:00 LT and lasted until $\sim$ 22:30 LT. We alternately obtained rain and air samples during that period. Similar to the gas phase, the rainwater contained H_2O_2, MHP, and PAA as the dominant peroxides. The time series of the different peroxides are shown in Fig. 4.

Interestingly, a negative correlation was observed between the time series for H_2O_2 and PAA in rainwater (see Fig. 4a), whereas the concentrations of gaseous H_2O_2 and PAA (Fig. 4b) still showed a positive correlation, similar to that on sunny days. Comparisons between the calculated and observed concentrations of peroxides in rainwater are shown in Fig. 4c, d, and e for H_2O_2, MHP, and PAA, respectively. The aqueous concentrations of peroxides are calculated on the basis of their gas phase concentrations and their effective Henry's law constants (K_H^*). K_H^* could be calculated with the physical Henry's law constants (K_H) reported by O'Sullivan et al. (1996) and the acidic dissociation constant (pKa) using Eq. (7):

$$K_H^* = K_H(1 + 10^{pH-pKa}). \quad (7)$$

The pKa is 11.6 for H_2O_2 (Marinoni et al., 2011) and 8.2 for PAA (Evans and Upton, 1985). This indicates that the K_H^* for H_2O_2 and PAA are almost equal to their K_H and are independent of the acidity in the pH range of rainwater, pH

Table 2. Dry deposition velocities for peroxides reported in the literature.

Peroxides	Region	v_d^a (cm s^{-1})	Note[b]	Reference
H_2O_2	Canadian boreal forest	5.0	daytime	Hall and Claiborn (1997)
		1.0	nighttime	Hall and Claiborn (1997)
H_2O_2	Cumberland plume	2.0	$H^c_{PBL} = 1425$ m	Jobson et al. (1998)
H_2O_2	Berlin-Brandenbury	0.1–4.4		Hammer et al. (2002)
H_2O_2		0.33–1.57	model result	Zhang et al. (2002)
H_2O_2	marine boundary layer	1.8 ± 0.6		Weller et al. (2000)
H_2O_2	ocean/rainforest	1.35	model result	Stickler et al. (2007)
H_2O_2	Norway spruce forest in Germany	5.0 ± 2.0	daytime	Valverde-Canossa et al. (2006)
ROOH	Canadian boreal forest	1.6	daytime	Hall and Claiborn (1997)
		0.5	nighttime	Hall and Claiborn (1997)
MHP	marine boundary layer	1.2 ± 0.4		Weller et al. (2000)
MHP	Norway spruce forest in Germany	1.0 ± 0.4	daytime	Valverde-Canossa et al. (2006)
ROOH/$H_2O_2^d$	Canadian boreal forest	0.28–0.61		Hall et al. (1999)

[a] v_d: deposition velocity, [b]PBL height is 1000 m without special notes, [c]H_{PBL}: the height of PBL, [d] the ratio of ROOH deposition velocity to H_2O_2 deposition velocity, dimensionless.

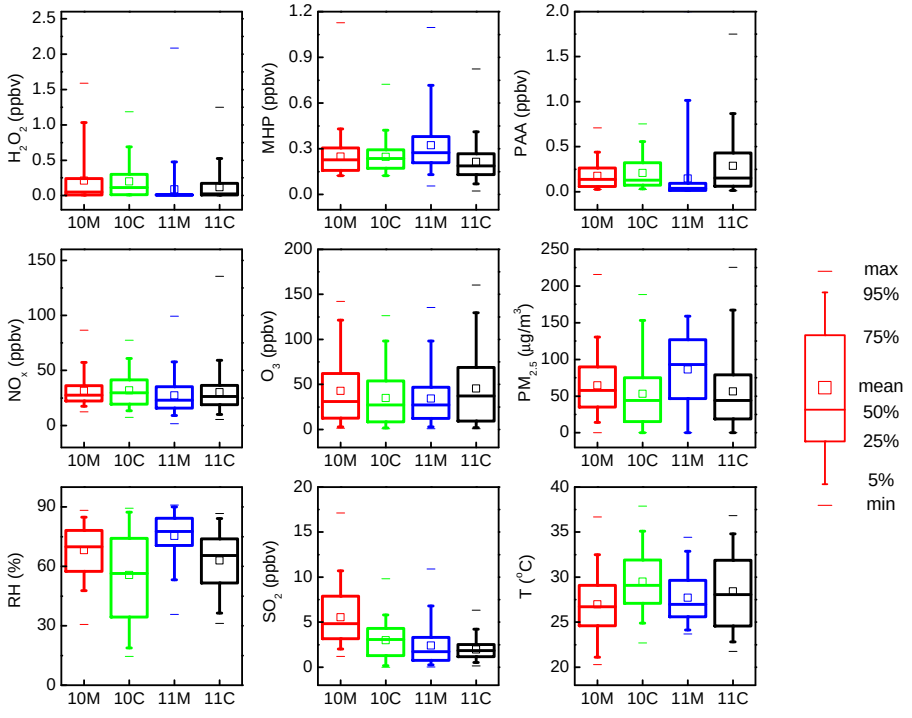

Fig. 3. Statistics for concentrations of peroxides, NO_x, O_3, $PM_{2.5}$, relative humidity (RH), SO_2, and temperature at marine and continental air mass sectors during August 2010 and August 2011. 10M: marine sector of August 2010; 10C: continental sector of August 2010; 11M: marine sector of August 2011; 11C: continental sector of August 2011.

= 4–7 (Xu et al., 2012); this has also been demonstrated in a laboratory study (Huang and Chen, 2010). It turned out that H_2O_2 is underpredicted at the beginning of the rain (Fig. 4c), as is PAA at the middle and ending stages of the rain (Fig. 4e). This underprediction suggests that there must be an extra source of aqueous peroxides besides scavenging from the gas phase. During this rain event, two possible sources are expected, namely the washout process of aerosol phase peroxides or the aqueous phase production in the rainwater. Previous laboratory studies (Arellanes et al., 2006; Shen et al., 2011; Y. Wang et al., 2010; Wang et al., 2011, 2012) have demonstrated that H_2O_2 could be generated in the aerosol phase by the decomposition of SOA particles and the redox reactions catalyzed by a small set of transition metal ions (TMI). In the real atmosphere, however, most of the aerosol-generated H_2O_2 would be quickly released to the

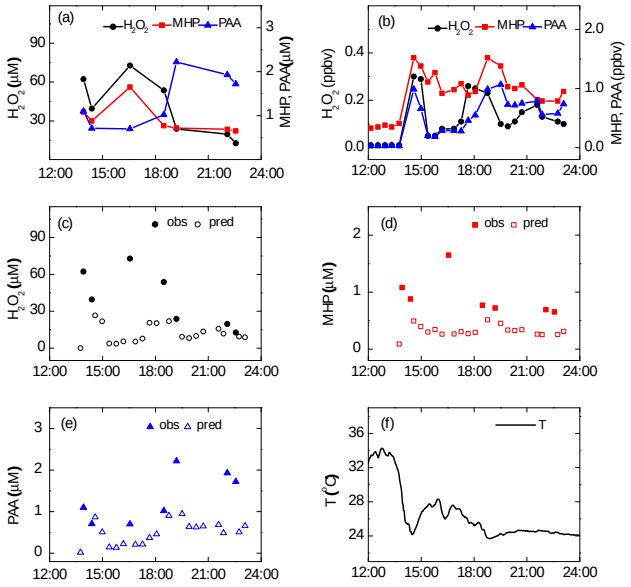

Fig. 4. Time series of gas phase and rainwater peroxides on 24 July 2011. **(a)** Observed peroxides in rainwater. **(b)** Observed peroxides in the gas phase. **(c)**–**(e)** Comparisons of gas phase peroxides observed (solid symbol) and predicted (open symbol) based on Henry's law. **(f)** Temperature.

ambient air to maintain the equilibrium between the aerosol and gas phases. Therefore, the H_2O_2 generated in aerosol could not accumulate fast enough to provide a stable source of H_2O_2 in the rainwater; this is also the case for PAA.

A more likely reason for the underprediction is the aqueous phase production. To account for the negative correlation between H_2O_2 and PAA, these two species should be produced at different stages of the rainfall. The aqueous phase production of H_2O_2 from the reaction of HO_2 and its conjugate base O_2^- (Reaction R8) is well established from previous laboratory and modeling studies (e.g., Anastasio et al., 1997; Jacob, 2000; Kim et al., 2002), and it also has been confirmed by long-term field measurements (Möller, 2009).

$$HO_2 + O_2^- + H^+ \rightarrow H_2O_2 + O_2 \quad \text{(R8)}$$

In a moderate acidic solution, the production rate of H_2O_2 from this reaction has been proven to be much faster than that from a self-reaction of HO_2 in the gas phase. We propose that this reaction is the cause of the aqueous phase H_2O_2 underprediction at the beginning of the rainfall period. The aqueous phase production of PAA occurs in two potential pathways. The first is the reaction of $CH_3C(O)O_2$ with O_2^- or $HC(O)O^-$ (Schuchmann and von Sonntag, 1988; Faust et al., 1997):

$$CH_3C(O)OO + O_2^- + H^+ \rightarrow CH_3C(O)OOH + O_2 \quad \text{(R9)}$$

$$CH_3C(O)OO + HC(O)O^- \rightarrow CH_3C(O)OOH + C(O)O^- \quad \text{(R10)}$$

$$C(O)O^- + O_2 \rightarrow CO_2 + O_2^- . \quad \text{(R11)}$$

$CH_3C(O)O_2$ could have been yielded from the OH-initiated reaction of acetaldehyde and the photolysis of biacetyl (Faust et al., 1997). However, this mechanism can explain the production of PAA but not the consumption of H_2O_2. The second potential pathway is the reversible reaction of H_2O_2 and acetic acid (AA). If this reaction is fast enough, it can explain the simultaneous consumption of H_2O_2. In the sulfuric acid solution, the rate constant for this reaction is estimated to be $3.6 \times 10^{-5}\,M^{-1}\,s^{-1}$ at 293 K (Dul'neva and Moskvin, 2005). This indicates that this reaction is of little significance unless the concentrations of H_2O_2 and AA are on the order of several mM or higher. In rainwater, H_2O_2 was determined at a maximum of $\sim 60\,\mu M$ in the present study; AA was not determined in the present study but has been reported at $\sim 2\,\mu M$ in previous studies (Xu and Han, 2009; Willey et al., 2011). The net PAA production rate is estimated to be only $\sim 1.6 \times 10^{-5}\,\mu M\,h^{-1}$, which is not sufficient to provide the extra source of PAA. Nevertheless, rainwater is a complicated system, and some catalytic mechanisms could exist for this reaction in the presence of reactive species including TMI, although as yet there is no laboratory evidence. Still, other unknown mechanisms leading to the conversion between H_2O_2 and PAA cannot be excluded. Additional analyses of the rainwater composition as well as laboratory kinetic studies should be performed to verify the exact mechanism.

3.3 Peroxides on haze days

We investigated a full haze episode in summer 2011, which is shown in Fig. 5. The haze arose at noontime on 10 August, and lasted until nighttime on 15 August. In the morning of 10 August, the mass concentration of $PM_{2.5}$ was around $30\,\mu g\,m^{-3}$ or less, a low level for Beijing. The $PM_{2.5}$ concentration increased at midday and maintained a high level over the following days; for example, its hourly averaged value reached $200\,\mu g\,m^{-3}$ on 12 August and $167\,\mu g\,m^{-3}$ on 13 August. The CO concentration was greatly enhanced, reaching a maximum of 2.4 ppmv (parts per million by volume), showing that the diffusion condition on those days was quite poor.

On 10 and 11 August, the beginning of the haze episode, low H_2O_2 and high PAA levels were observed. On the following haze days, however, both the H_2O_2 and PAA levels decreased to near or under the detection limit. The diurnal profile of MHP for haze days, peaking at midnight and decreasing rapidly in the daytime, was distinct from that for non-haze days, although its mean concentration, ~ 0.26 ppbv, varied only a little. Although SO_2, NO_x, and water vapor have been proven to be responsible for the decrease in peroxides, their concentrations showed little difference between non-haze and haze days. High NO_x was regarded as the largest suppression of

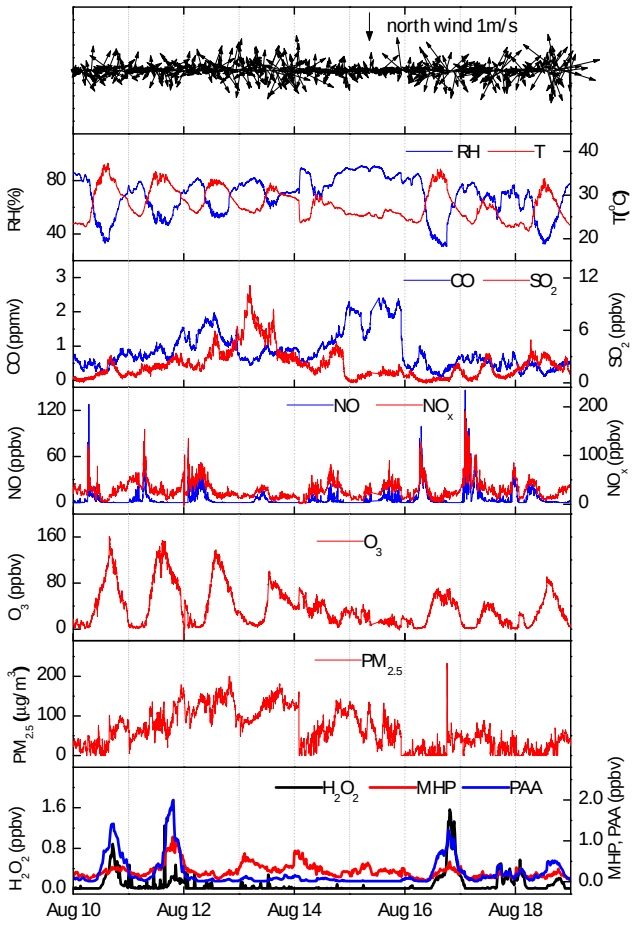

Fig. 5. Time series of observed meteorological parameters, SO_2, CO, NO, NO_x, O_3, $PM_{2.5}$ and peroxides on 10–18 August 2011 (during and after the haze episode).

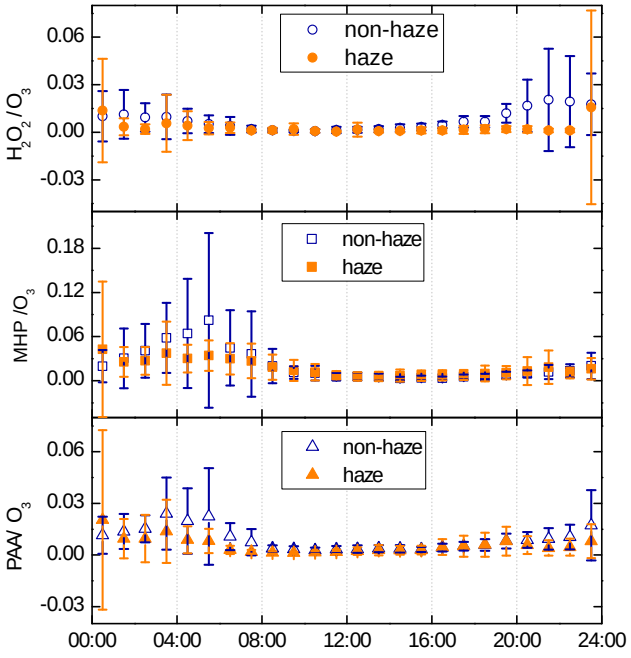

Fig. 6. Hourly-averaged ratio of peroxide to O_3 on non-haze and haze days. The error bar represents the standard deviation (1σ) of the 1 h average data.

peroxide formation. However, NO_x (27.9 ± 15.0 ppbv) on haze days was even slightly lower than it was on non-haze days (30.6 ± 14.1 ppbv). Moreover, there were few clouds and low-speed winds during both observation periods, indicating that the decrease in peroxides was neither due to the decline of solar radiation caused by increasing clouds nor due to the horizontal transport with the wind. Therefore, we tentatively ascribe this decrease in peroxides to the impact of enhanced aerosols. Aerosols can play a dual role in peroxide chemistry, as mentioned in Sect. 1. First, aerosols attenuate the solar radiation and subsequently weaken the photochemical activity of trace gases. This attenuation can be evaluated by the aerosol optical depth (AOD), which represents the extinction of solar radiation through aerosol scattering and absorption. AOD has been proven to increase linearly with increasing $PM_{2.5}$ mass concentration, especially in metropolitan areas (Chu, 2006; Schaap et al., 2009). Therefore, increasing $PM_{2.5}$ can result in an increasing AOD and reduced solar radiation. In addition, the low ozone that was observed on haze days also provides evidence for weakened photochemical processes. As a result, both the photochemical production and the photolysis of H_2O_2 were weakened. Second, aerosols provide sites for heterogeneous reactions. These reactions can provide either sources or sinks for peroxides. In the real atmosphere, however, these two impacts of aerosols are in fact mixed and interactive. A simple means of distinguishing them is to compare the ratio of peroxide to ozone (PO/O_3) on the non-haze and haze days. Ozone has similar photochemical processes with peroxides but is little affected by the heterogeneous reaction occurring on aerosols (Jacob, 2000; Mogili et al., 2006). Thus, the variability of PO/O_3 could reflect how much the heterogeneous reaction affects peroxides. Because peroxides have a different diurnal cycle than ozone, PO/O_3 is lowest at noontime and highest in the late afternoon. As shown in Fig. 6, the highest value of PO/O_3 on non-haze days was higher than the highest value on haze days, particularly for H_2O_2. This suggests that the heterogeneous reaction provided a sink for peroxides. Nevertheless, any conclusion based solely on the PO/O_3 ratio would be preliminary and possibly inaccurate, because the sensitivity to the solar radiation is in fact different between peroxides and ozone. Although both peroxides and ozone are produced by the reactions of peroxy radicals, the production rate of peroxides is quadratic on the concentrations of peroxy radicals, whereas the production rate of ozone is linear (Ran et al., 2012). Model calculations are required to further verify the impacts of aerosols on peroxides. The model calculations are described in Sect. 3.4.

3.4 Modeling

3.4.1 Standard gas phase model

We use a photochemical box model based on the NCAR_MM mechanism to quantify the impacts of aerosols on peroxides. Details on this model are provided in Sect. 2.4. The model did not reproduce MHP and PAA well due to the lack of VOC measurement data and their unclear heterogeneous reaction mechanisms. Here we focus on the simulation of H_2O_2.

The model runs begin every thirty minutes. The observed concentrations of CO, NO, NO_2, H_2O, and O_3 are used as input data to initialize each model run. The small amount of data missing due to the instrument problem is filled through interpolation. It is unfortunate that the detailed VOC (volatile organic compound) data for the investigated two summers are unavailable. As an alternative, we use the daily mean values of the VOCs observed during summer 2007 (Liu et al., 2012) as input data to the model. The lack of VOC measurements would result in a considerable uncertainty for simulating H_2O_2 and a poor simulation for MHP and PAA. However, some information can be used to understand the year to year variability in VOC levels as well as the variability between non-haze and haze days. B. Wang et al. (2010) reported that the vehicle emission was the major source for NMHCs (non-methane hydrocarbons) in summer Beijing. Lang et al. (2012) analyzed the variation trend of vehicle population and vehicular emission factors in Beijing from 1999 to 2010. In their study, the vehicle population in Beijing increased but the emission factors decreased year by year. As a result, the NMHC emissions showed a slight decreasing trend, decreasing $\sim 15\,\%$ in year 2010 compared to year 2007. We made a NMHC comparison between the haze episode (summer 2006 reported by Guo et al., 2012) and the normal days (e.g., summer 2007 reported by Liu et al., 2012) and found no significant difference in concentrations and distribution of different types of NHMCs. Therefore, we suggest that the change for VOCs in Beijing would be expected to a small extent from 2007 to 2011 and between non-haze and haze days. The concentrations of output products are input into the next model run. The initial value of H_2O_2 is given by its observed value at 00:00 LT each day. The height of the planetary boundary layer (PBL) over Beijing is assumed to fluctuate between 500 m and 1500 m, with the maximum at noon and the minimum at midnight (Sun et al., 2012). In the TUV model, the wavelength is assumed to range from 120 nm to 735 nm, and the single scattering albedo is assumed to be 0.90 (Xia et al., 2006). The model uses the AOD at 550 nm (AOD_{550}) as an input parameter, which is calculated as follows: $AOD_{550} = [PM_{2.5}(\mu g\,m^{-3}) - 25.85]/45.57$ (Lin et al., 2013). The dry deposition rate of H_2O_2 is set as $1.8 \times 10^{-5}\,s^{-1}$ at a PBL height of 1000 m, which is a moderate rate as discussed in Sect. 3.1.

Before simulating the observed H_2O_2, we conduct sensitivity analyses in eight cases to investigate the effects of the different input parameters on H_2O_2. The date of 7 August 2010 is selected for these analyses. The analyzed compounds include CO, NO, NO_2, H_2O, O_3 and the categorized VOCs (alkanes, alkenes, and aromatics). In each case, we reduced one of these compounds by half compared to the reference run and then calculated the concentrations of OH, HO_2, and H_2O_2. The modeled daytime maximum concentrations of OH, HO_2, and H_2O_2 are compared in Table 3. It is seen that the H_2O_2 concentration is most sensitive to NO_2 but it is insensitive to NO. In the daytime, the self-reaction of HO_2, which produces H_2O_2, competes with the HO_2+NO reaction. Meanwhile, there is a rapid conversion between NO_2 and NO, and as a result, both NO_2 and NO can equally suppress the formation of H_2O_2. Because the daytime concentration of NO_2 is usually much greater than that of NO, H_2O_2 is far more sensitive to NO_2 than NO for the same percentage change. In addition to NO_2, H_2O_2 is also sensitive to water vapor, which catalyzes the self-reaction of HO_2 (Sander et al., 2011), and to the aromatics that greatly affect the formation of HO_2. In the NCAR_MM mechanism, the aromatics are assumed to perform ring opening reactions that yield organic compounds with a lower carbon number. This process produces a large amount of oxygenated VOCs (OVOCs), which sequentially provide primary sources for HO_2. Therefore, the input aromatics are responsible for the largest uncertainty in the model simulation. However, as these aromatics are mainly emitted by vehicles in Beijing (Y. J. Zhang et al., 2012), we can presume that their level in August 2010 is similar to their level in August 2011. The vehicle population at the end of 2011 was 4.983 million compared with 4.809 million at the end of 2010; this is an increment of only 3.6 % (http://www.bjjtgl.gov.cn). This low increment is attributed to a policy implemented at the end of 2010 that limits new vehicle registrations. In addition, the meteorological conditions in August 2011 were similar to those in August 2010. Therefore, a comparison of the simulation results between August 2011 and August 2010 is valuable. The aerosols could alter the solar radiation intensity, resulting in a variation of HO_x and H_2O_2. A sensitivity analysis for HO_x and H_2O_2 to AOD was made, and the result is shown in Table S2 in the Supplement. It is seen that both HO_x and H_2O_2 were more sensitive to AOD at a lower AOD (< 2). This could be explained by the dual role of solar radiation, that is, it impacts on both the source and loss of HO_x and H_2O_2.

Figure 7 shows the concentrations of H_2O_2 both observed and calculated by the standard gas phase model. It turns out that the model has good performance simulating non-haze days, except it underestimates the nighttime removal rates. This underestimation is due to the preference for dry deposition velocity, as discussed in Sect. 3.1. The level of H_2O_2 on haze days, however, is significantly underestimated even though the extinction effect of aerosols has been corrected by AOD. Therefore, this underestimation of H_2O_2

Table 3. Calculated concentrations of OH, HO_2, and H_2O_2 for sensitivity analyses when the concentration of each trace gas in column 1 has been reduced by half.

Model run	OH (pptv)	HO_2 (pptv)	H_2O_2 (ppbv)
reference run	0.37	25.5	0.70
CO	0.38	23.5	0.60
H_2O	0.29	20.6	0.32
NO	0.38	27.8	0.78
NO_2	0.42	54.1	4.19
O_3	0.41	22.0	0.46
alkanes	0.38	25.9	0.72
alkenes	0.36	20.6	0.52
aromatics	0.23	8.5	0.10

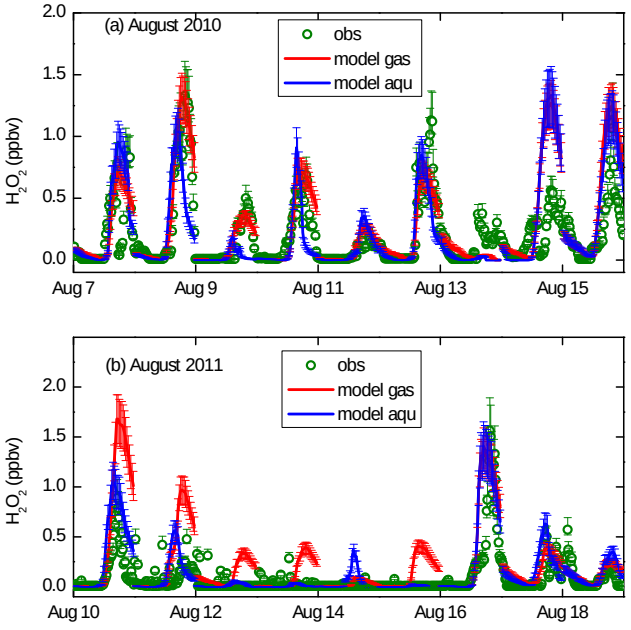

Fig. 7. Observed and modeled H_2O_2 concentrations on 7–15 August 2010 and 10–18 August 2011. Green circles: observed H_2O_2; red line: modeled H_2O_2 with standard gas phase chemistry; blue line: modeled H_2O_2 with the inclusion of aqueous phase chemistry. The error bar for observed data represents the uncertainty caused by instrument fluctuation and SO_2 interference; the error bar for modeling data represents the uncertainty (1σ) caused by the uncertainty of concentrations of the constrained species.

concentrations should be attributed to the heterogeneous reaction occurring on aerosols.

3.4.2 Treatment of aerosol uptake

The aerosol uptake of HO_2 was considered to be responsible for the overestimation of observed H_2O_2 in previous studies (Cantrell et al., 2003; Wang et al., 2003; de Reus et al., 2005; Mao et al., 2010). This may also be true over urban Beijing where the aerosol loading is considerably high. The most common method of representing HO_2 uptake in the model is to include an uptake coefficient of HO_2 (γ_{HO_2}), with or without products (Wang et al., 2003; Mao et al., 2010). However, this may not be reasonable for a local scale simulation because the value of γ_{HO_2} significantly depends on changing conditions. Therefore, HO_2 uptake could be more reliably represented if certain specific reactions are properly included in the model. However, the mechanism and products for HO_2 uptake remain uncertain. It is generally accepted that after being taken up by aerosols, HO_2 will dissociate in the aerosol aqueous phase into O_2^- and it will subsequently produce H_2O_2 (Jacob, 2000). Yet, the inclusion of this mechanism leads to an increase of gaseous H_2O_2, which the overestimation in the present study would exacerbate. There are some mechanisms suggesting that HO_2 could ultimately be converted to H_2O, thus leading to a net loss of gaseous HO_2 and H_2O_2. For example, Cooper and Abbatt (1996) proposed that HO_2 could react with HSO_4^- and form the peroxymonosulfate radical SO_5^-; also, Matthew et al. (2003) put forward a mechanism by which HO_2 could be consumed by some reactive halogen species. Both mechanisms could result in the net loss of HO_2 to a certain extent. Nevertheless, they are not catalytic and could easily reach equilibration; thus, they may not greatly affect the concentration of H_2O_2 in the real atmosphere. Quite recently, Mao et al. (2013) proposed a catalytic mechanism involving TMI chemistry. In their mechanism, HO_2 uptake will lead to either the production or the consumption of H_2O_2, depending on the molar ratio of Cu to Fe. We believe this mechanism plays an important role in summer Beijing because the concentrations of aerosol Cu and Fe are high and the ratio of Cu to Fe in $PM_{2.5}$ (Sun et al., 2004, 2006) is in the expected range of the mechanism. Therefore, we add the relevant reactions to the box model as well as some other basic aqueous phase reactions that are drawn from the aqueous phase CAPRAM v2.4 mechanism. We then examine the impacts of these reactions on the HO_2 and H_2O_2 concentrations during both non-haze days and haze days.

The Cu-Fe-HO_x catalytic mechanism may not fully represent the reaction process in the real atmosphere, as the aqueous phase reactions of some organic species are involved and the reaction process could change (Mao et al., 2013). Moreover, the reactive uptake of HO_2 and H_2O_2 could also occur on the surface of solid aerosols. Due to the lack of adequate information, the aqueous reactions of organics and the uptake of H_2O_2 and HO_2 on solid surfaces are not included in the present study.

3.4.3 Inclusion of the Cu-Fe-HO_x catalytic mechanism

How the Cu concentration, molar Cu / Fe ratio and pH impact on γ_{HO_2} and H_2O_2 yield should be evaluated before starting the simulation of H_2O_2. Here, sensitivity analyses for these factors are performed. The sensitivity simulations

are conducted at noontime when the generation of H_2O_2 is strongest, and they last for 4 h. For each simulation, the initial concentrations of CO, H_2O_2, NO, NO_2, and O_3 are 1 ppmv, 1 ppbv, 2 ppbv, 20 ppbv, and 30 ppbv, respectively, and the initial concentrations of the VOCs are the same as those in the standard gas phase simulations. The H_2O_2 concentrations at the end of each simulation are compared. Figure 8a shows the impact of Cu / Fe on the H_2O_2 concentration at different LWC levels. It is seen that the aqueous phase reactions will be almost independent of the Cu / Fe ratio when LWC $< 10\,\mu g\,m^{-3}$ or $> 100\,\mu g\,m^{-3}$. At high LWC ($> 100\,\mu g\,m^{-3}$), HO_2 enters the aerosol aqueous phase and is consumed rapidly, resulting in low HO_2 in both gas and aqueous phase. Thus, TMI in the aqueous phase is sufficient to convert HO_2 and H_2O_2 to H_2O, leading to a very low H_2O_2 level. In contrast, at low LWC ($< 10\,\mu g\ m^{-3}$), HO_2 concentration is high and TMI is insufficient to convert HO_2 to H_2O but instead produce H_2O_2 in small amounts. However, at an LWC level of 25–50 $\mu g\,m^{-3}$, the H_2O_2 concentration is dependent on Cu / Fe. In particular, the H_2O_2 concentration remarkably increases with increasing Cu / Fe when Cu / Fe $> 10^{-2}$, as Cu reaction dominates over Fe reaction. Figure 8b illustrates that the H_2O_2 concentration has a weak pH dependence. The initial concentration of H^+ does not significantly affect the reactions compared to the produced H^+ because the pH is not held fixed throughout each simulation. Figure 8c shows the sensitivity of the aqueous phase reactions toward the dissolved Cu concentration at a fixed Cu / Fe of 0.02. It turns out that the calculated H_2O_2 decreases with increasing Cu when the Cu concentration is greater than 1×10^{-3} M due to the consumption of HO_2 by sufficient TMIs.

We use the Cu-Fe-HO_x catalytic mechanism to simulate H_2O_2 on both non-haze and haze days. The liquid water content on the aerosols is calculated using the single-parameter method reported in Kreidenweis et al. (2008), on the basis of the measured mass concentrations of $PM_{2.5}$ and the components of particles reported by Sun et al. (2004). The surface area of the aerosols is calculated based on their size distribution and the geometric shape of one aerosol particle, which is assumed to be spherical. We estimated the surface area of the aerosols to be 800 $\mu m^2\,cm^{-3}$ for non-haze days and 2400 $\mu m^2\,cm^{-3}$ for haze days, using the size distribution of aerosols in summer Beijing reported by Yue et al. (2009), as well as the calibration with diameter growth factors (Kreidenweis et al., 2008). Due to the metastability of the aqueous phase (S. T. Martin et al., 2003) and the decreased deliquescence RH for the mixed aerosols (e.g., Marcolli et al., 2004), the aerosols are expected to remain aqueous over the RH range experienced during our observations. Therefore, the surface area could be assumed to be primarily due to the aqueous aerosols. The aerosol radius used in Eqs. (4) and (5) is the surface area weighted average radius, which is 140 nm for non-haze days and 200 nm for haze days. The pH is set to 5.48 (Wang et al., 2005) at the beginning of each

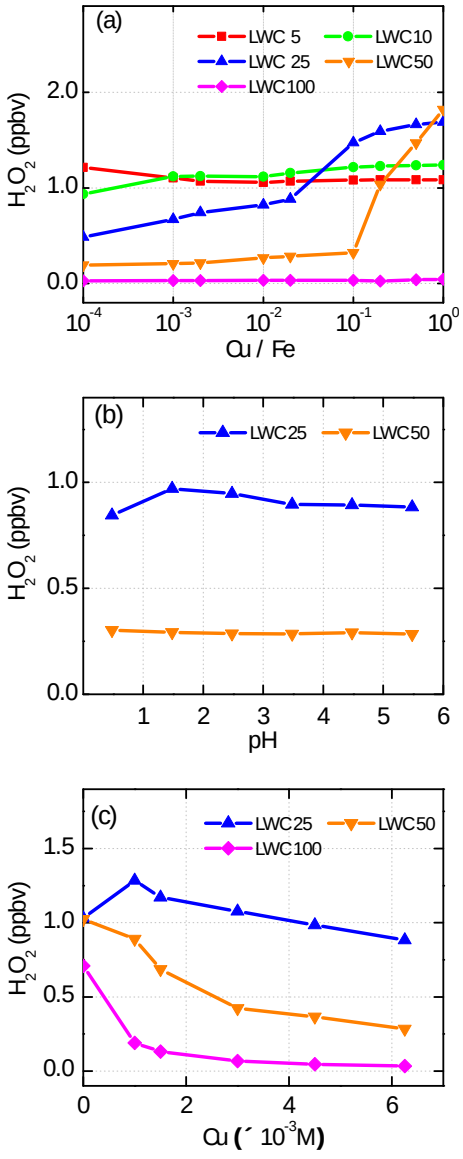

Fig. 8. Impacts of aerosol aqueous phase Cu / Fe, pH, and Cu concentration on gaseous H_2O_2 concentrations at different LWC levels ($\mu g\,m^{-3}$). **(a)–(b)** Cu concentration is held fixed at 6.25×10^{-3} M. **(b)–(c)** Cu / Fe is held fixed at 0.02.

model run. We hold the dissolved Cu concentration fixed at 6.25×10^{-3} M and Cu / Fe at 0.02, according to the total observed concentration in $PM_{2.5}$ (Sun et al., 2004, 2006) and the assumption that Cu and Fe are dissolved by half. Figure 7 shows the results for the simulation. With the inclusion of the aqueous phase reactions, the H_2O_2 concentration on non-haze days does not change much and there is an improvement in the reproduction of its removal rates at night for most of the days. This implies that the aqueous reactions could compensate for the missing removal pathway to some extent at night. There is a greater coincidence between the observed and modeled H_2O_2 concentrations on haze days,

which indicates that the aqueous phase reactions play an important role in the loss of H_2O_2 on haze days. On non-haze days, the aqueous phase reactions are only important at night when the RH is high. On haze days, the higher aerosol liquid water content favors the uptake of HO_2 and the consumption of aqueous phase H_2O_2, during both daytime and nighttime.

3.4.4 HO_2 and H_2O_2 budget

Based on the model results, we developed the budget of HO_2 and H_2O_2 for non-haze (7–15 August 2010) and haze days (10–15 August 2011), respectively, as shown in Fig. 9. The following can be seen in the gas phase: (1) the photolysis of OVOCs provides a primary source for HO_2; (2) the major cycling system for HO_2 includes the conversions of HO_2 to OH, RO_2 to HO_2, and OH to HO_2; and (3) the formation of H_2O_2 and organic peroxides and the aerosol uptake serve as important removal pathways for HO_2. On non-haze days, there are high rates of formation and recycling for gaseous HO_2 due to its abundant primary source; on haze days, however, these rates decrease considerably and are only one third of the values for non-haze days. This is due to the lower concentrations of gaseous HO_2 and OH on haze days, resulting from the lower radiation and the stronger aqueous phase removal.

In the aqueous phase, HO_2 has a major source, the uptake from the gas phase, and a minor source, the aqueous Cu(I)+O_2 reaction (not shown in Fig. 9). The aqueous HO_2 could either release into the gas phase or react with Cu(II) and Fe(II) and thus be consumed. The removal rate of HO_2 is then determined by the difference between the uptake and volatilization rates. As shown in Fig. 9, the HO_2 uptake rate is apparently higher than its volatilization rate on both non-haze and haze days, indicating HO_2 is significantly consumed in the aqueous phase. H_2O_2 is the product of aqueous reactions of HO_2 and could be consumed by Fe(II) and S(IV) in the aqueous phase. The consumption of H_2O_2 by dissolved S(IV), with a rate lower by a factor of 30–60, is not comparable with TMI catalytic reactions due to the insufficient LWC on non-haze days and the low concentrations of gaseous H_2O_2 on haze days. However, the H_2O_2+S(IV) reaction could compete with TMI catalytic reactions at certain time points when the LWC is particularly high, e.g., above 200 $\mu g\,m^{-3}$. The exchange rate of H_2O_2 between the gas and aerosol phases is on the order of dozens of ppbv h^{-1}, which is much faster than other processes. This rate almost doubles on haze days compared to non-haze days, although gaseous H_2O_2 on haze days is often under the detection limit. The uptake rate of H_2O_2, however, is equal to or less than the volatilization rate, reflecting the lack of net reactive uptake of H_2O_2. This reveals a balance between the production and consumption of H_2O_2 in the aqueous phase. Provided that there is no aqueous production of H_2O_2, the consumption of H_2O_2 by Fe(II) and S(IV) will lead to a reactive uptake of H_2O_2 with an uptake coefficient of $(1–2)\times10^{-3}$. This approaches the uptake coefficient for H_2O_2 on mineral dust, $(3.3–9.4)\times10^{-4}$, which was measured in a laboratory by Pradhan et al. (2010a, b).

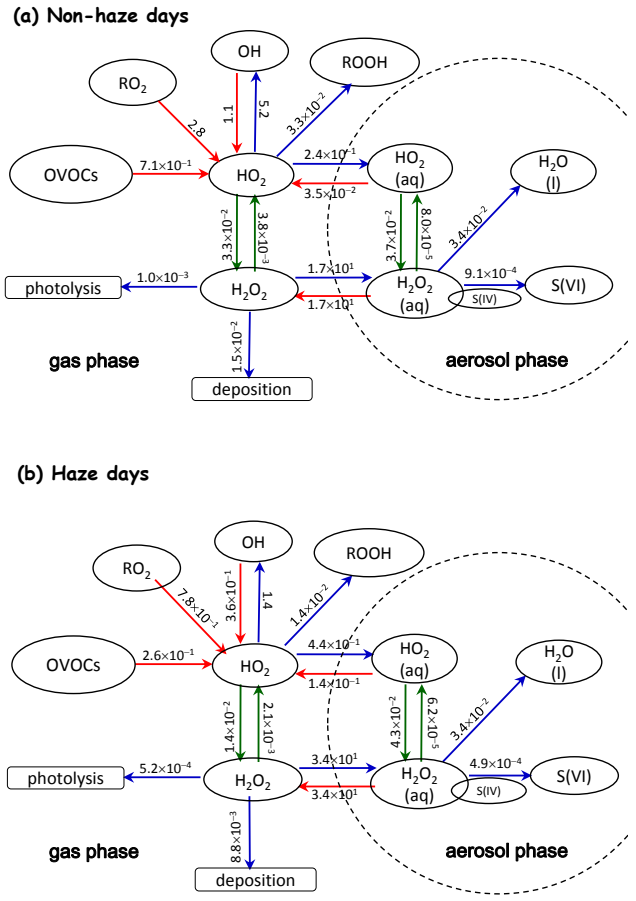

Fig. 9. 24 h average OH and HO_2 budget on **(a)** non-haze days and **(b)** haze days. Red arrows refer to the sources of HO_2, blue arrows refer to the sinks of HO_2 and H_2O_2, and green arrows refer to the conversion between HO_2 and H_2O_2. All rates are in ppbv h^{-1}. The rates for aqueous phase reactions are converted to ppbv h^{-1} according to the number of molecules per unit volume. HO_2(aq) refers to the sum of aqueous phase HO_2 and O_2^-. The average aerosol liquid water content is $\sim34\,\mu g\,m^{-3}$ for non-haze days and $\sim71\,\mu g\,m^{-3}$ for haze days.

According to Mao et al. (2013), the aqueous phase removal of HO_2 and the simultaneous variation of aqueous H_2O_2 could be described as $\gamma(HO_2 \rightarrow Y_{H_2O_2}\ H_2O_2)$ on the basis of the HO_2 and H_2O_2 budget. γ is the average reactive uptake coefficient, which reflects the possibility of aqueous reactions of HO_2 after uptake by the aerosols. The $Y_{H_2O_2}$ is defined here as the net yield of H_2O_2, reflecting the formation potential of aqueous H_2O_2 through the uptake of HO_2. Interestingly, we find that the average reactive uptake coefficient of HO_2 for non-haze days is 0.86, which is higher than the value of 0.68 on haze days. This could be attributed to the faster aqueous phase diffusion in smaller aqueous aerosols

and different HO_2-dependent chemical conversions on non-haze days compared to haze days. We estimated the characteristic times of aqueous phase diffusion (τ_{diff}) and chemical reactions (τ_{chem}) for HO_2 according to the equations given by Jacob (2000), and found that both τ_{diff} and τ_{chem} were on the same order. This indicates that γ_{HO_2} would be determined by the combination of both processes. However, the $Y_{H_2O_2}$ on haze days, with a value of -0.004, is significantly lower than the value of 0.059 on non-haze days, resulting in a more remarkable reduction of gaseous H_2O_2. Note that the uptake coefficients of HO_2 needed on both non-haze and haze days seem too high compared to the experimentally measured values (from <0.01 to 0.40), suggesting that there should be some unknown processes going on.

4 Summary and conclusions

We measured atmospheric peroxides over urban Beijing in August 2010 (non-haze days) and August 2011 (haze days). Hydrogen peroxide (H_2O_2), methyl hydroperoxide (MHP), and peroxyacetic acid (PAA) were determined to be the three major peroxides during both of these summers. Combining the supporting data from common gases and meteorological parameters, we analyzed the peroxides and HO_2 radicals statistically, and using a box model, focused on how they are affected by aerosols.

A negative correlation was observed between H_2O_2 and PAA in rainwater, reflecting the conversion of H_2O_2 to PAA in the aqueous phase. We attribute this conversion to a reversible reaction of H_2O_2 with acetic acid (AA). However, the rate of this reaction is insufficient to meet the observed the rate of PAA production, indicating that there should be some catalytic mechanism for this reaction in the rainwater. Moreover, the possibility of some unknown reaction mechanisms cannot be excluded. Obviously, further field and laboratory studies are needed to verify the exact mechanism of PAA production in the aqueous phase.

The average H_2O_2 concentration on haze days is only about 30 % greater than on non-haze days. We attribute this reduction in H_2O_2 to the attenuation of solar radiation as well as the enhanced heterogeneous reaction occurring on aerosols during the haze episodes. An NCAR_MM box model was employed to simulate the temporal profiles of H_2O_2 on non-haze and haze days. The model performs well on non-haze days but significantly overpredicts H_2O_2 on haze days. The discrepancy between the observed and modeled H_2O_2 apparently diminishes when we included a newly proposed Cu-Fe-HO_x catalytic mechanism. The combination of observed and modeled results of H_2O_2 suggests that the aerosol uptake of HO_2 and the ensuing aqueous reactions are major reasons for the reduction of H_2O_2 on haze days. According to the closure of H_2O_2 and HO_2, the average uptake coefficient for HO_2 (γ_{HO_2}) on aerosols is estimated to be 0.86 on non-haze days and 0.68 on haze days, and the corresponding net yield of H_2O_2 by HO_2 is 0.059 and -0.004, respectively. The γ_{HO2} needed to meet the measurements is too high compared to the experimentally measured values, indicating some other processes must be going on. For both non-haze and haze days, the consumption of H_2O_2 by S(IV) on aerosols is shown to be unimportant under normal conditions for urban Beijing.

We suggest that there is almost no net reactive uptake for H_2O_2 on aerosols because of the coexistence of HO_2 uptake. The production of H_2O_2 via the aerosol uptake of HO_2 from the gas phase is typically in balance with the consumption of H_2O_2 on aerosols. However, this balance could be broken if there are more H_2O_2-consuming reactions. Therefore, kinetic studies focused on the aerosol uptake of gaseous H_2O_2 in the presence of gaseous HO_2 are urgently needed.

Moreover, we suggest that the exchange rate of H_2O_2 between the gas and aerosol phases is on the orders of dozens of ppbv h^{-1}, revealing the potential importance of H_2O_2 in aerosols, even when gaseous H_2O_2 is observed under the detection limit. This high exchange rate of H_2O_2 may be helpful in explaining why haze frequently occurs in Beijing as well as the North China region.

Supplementary material related to this article is available online at http://www.atmos-chem-phys.net/13/11259/2013/acp-13-11259-2013-supplement.pdf.

Acknowledgements. This work was funded by the National Natural Science Foundation of China (grants 41275125, 40875072). We gratefully thank L. M. Zeng and M. Hu (Peking University) for data support for the meteorological factors and common gases, the NOAA Air Resources Laboratory (ARL) for the provision of the HYSPLIT transport and dispersion model and READY website (http://ready.arl.noaa.gov), and the NCAR Earth System Laboratory (NESL) for the provision of the Master Mechanism box model used in this publication.

Edited by: M. Ammann

References

Anastasio, C., Faust, B. C., and Rao, C. J.: Aromatic carbonyl compounds as aqueous-phase photochemical sources of hydrogen peroxide in acidic sulfate aerosols, fogs, and clouds. 1. Non-phenolic methoxybenzaldehydes and methoxyacetophenones with reductants (phenols), Environ. Sci. Technol., 31, 218–232, doi:10.1021/es960359g, 1997.

Arellanes, C., Paulson, S. E., Fine, P. M., and Sioutas, C.: Exceeding of Henry's law by hydrogen peroxide associated with urban aerosols, Environ. Sci. Technol., 40, 4859–4866, doi:10.1021/es0513786, 2006.

Bedjanian, Y., Lelievere, S., and Le Bras, G.: Experimental study of the interaction of HO_2 radicals with soot surface, Phys. Chem. Chem. Phys., 7, 334–341, 2005.

Bedjanian, Y., Romanias, M. N., and El Zein, A.: Uptake of HO_2 radicals on Arizona Test Dust, Atmos. Chem. Phys., 13, 6461–6471, doi:10.5194/acp-13-6461-2013, 2013.

Böge, O., Miao, Y., Plewka, A., and Herrmann, H.: Formation of secondary organic particulate phase compounds from isoprene gas-phase oxidation products: an aerosol chamber and field study, Atmos. Environ., 40, 2501–2509, 2006.

Calvert, J. G., Lazrus, A. L., Kok, G. L., Heikes, B. G., Welega, J. G., Lind, J., and Cantrell, C. A.: Chemical mechanisms of acid generation in the troposphere, Nature, 317, 27–35, 1985.

Cantrell, C. A., Mauldin, L., Zondlo, M., Eisele, F., Kosciuch, E., Shetter, R., Lefer, B., Hall, S., Campos, T., Ridley, B., Walega, J., Fried, A., Wert, B., Flocke, F., Weinheimer, A., Hannigan, J., Coffey, M., Atlas, E., Stephens, S., Heikes, B., Snow, J., Blake, D., Blake, N., Katzenstein, A., Lopez, J., Browell, E. V., Dibb, J., Scheuer, E., Seid, G., and Talbot, R.: Steady state free radical budgets and ozone photochemistry during TOPSE, J. Geophys. Res., 108, 8361, doi:10.1029/2002jd002198, 2003.

Chameides, W. L., Yu, H., Liu, S. C., Bergin, M., Zhou, X., Mearns, L., Wang, G., Kiang, C. S., Saylor, R. D., Luo, C., Huang, Y., Steiner, A., and Giorgi, F.: Case study of the effects of atmospheric aerosols and regional haze on agriculture: An opportunity to enhance crop yields in China through emission controls?, Proc. Natl. Acad. Sci. USA, 96, 13626–13633, doi:10.1073/pnas.96.24.13626, 1999.

Chu, D. A.: Analysis of the relationship between MODIS aerosol optical depth and PM, Proceedings of SPIE, 6299, 629903–629909, doi:10.1117/12.678841, 2006.

Claeys, M., Wang, W., Ion, A. C., Kourtchev, I., Gelencsér, A., and Maenhaut, W.: Formation of secondary organic aerosols from isoprene and its gas-phase oxidation products through reaction with hydrogen peroxide, Atmos. Environ., 38, 4093–4098, 2004.

Cohan, D. S., Schultz, M. G., and Jacob, D. J.: Convective injection and photochemical decay of peroxides in the tropical upper troposphere: methyl iodide as a tracer of marine convection, J. Geophys. Res., 104, 5717–5724, 1999.

Cooper, P. L. and Abbatt, J. P. D.: Heterogeneous interactions of OH and HO_2 radicals with surfaces characteristic of atmospheric particulate matter, J. Phys. Chem., 100, 2249–2254, 1996.

de Reus, M., Fischer, H., Sander, R., Gros, V., Kormann, R., Salisbury, G., Van Dingenen, R., Williams, J., Zöllner, M., and Lelieveld, J.: Observations and model calculations of trace gas scavenging in a dense Saharan dust plume during MINATROC, Atmos. Chem. Phys., 5, 1787–1803, doi:10.5194/acp-5-1787-2005, 2005.

Draxler, R. R. and Rolph, G. D.: HYSPLIT (HYbrid Single-Particle Lagrangian Integrated Trajectory) Model access via NOAA ARL READY Website, available at: http://ready.arl.noaa.gov/HYSPLIT.php (last access: December 2012), NOAA Air Resources Laboratory, Silver Spring, MD, 2012.

Duan, J. C., Guo, S. J., Tan, J. H., Wang, S. L., and Chai, F. H.: Characteristics of atmospheric carbonyls during haze days in Beijing, China, Atmos. Res., 114, 17–27, 2012.

Dul'neva, L. V. and Moskvin, A. V.: Kinetics of formation of peroxyacetic acid, Russian J. Gen. Chem., 75, 1125–1130, 2005.

Ervens, B., George, C., Williams, J. E., Buxton, G. V., Salmon, G. A., Bydder, M., Wilkinson, F., Dentener, F., Mirabel, P., Wolke, R., and Herrmann, H.: CAPRAM 2.4 (MODAC mechanism): An extended and condensed tropospheric aqueous phase mechanism and its application, J. Geophys. Res., 108, D144426, doi:10.1029/2002jd002202, 2003.

Evans, D. F. and Upton, M. W.: Studies on singlet oxygen in aqueous solution, Part 3: The decomposition of peroxy-acids, J. Chem. Soc. Dalton Trans., 6, 1151–1153, 1985.

Faust, B. C., Powell, K., Rao, C. J., and Anastasio, C.: Aqueous-phase photolysis of biacetyl (An α-dicarbonyl compound): A sink for biacetyl, and a source of acetic acid, peroxyacetic acid, hydrogen peroxide, and the highly oxidizing acetylperoxyl radical in aqueous aerosols, fogs, and clouds, Atmos. Environ., 31, 497–510, doi:10.1016/s1352-2310(96)00171-9, 1997.

Feichter, J., Kjellström, E., Rodhe, H., Dentener, F., Lelieveldi, J., and Roelofs, G.-J.: Simulation of the tropospheric sulfur cycle in a global climate model, Atmos. Environ., 30, 1693–1707, doi:10.1016/1352-2310(95)00394-0, 1996.

Fleming, Z. L., Monks, P. S., Rickard, A. R., Heard, D. E., Bloss, W. J., Seakins, P. W., Still, T. J., Sommariva, R., Pilling, M. J., Morgan, R., Green, T. J., Brough, N., Mills, G. P., Penkett, S. A., Lewis, A. C., Lee, J. D., Saiz-Lopez, A., and Plane, J. M. C.: Peroxy radical chemistry and the control of ozone photochemistry at Mace Head, Ireland during the summer of 2002, Atmos. Chem. Phys., 6, 2193–2214, doi:10.5194/acp-6-2193-2006, 2006.

Frey, M. M., Stewart, R. W., McConnell, J. R., and Bales, R. C.:Atmospheric hydroperoxides in west Antarctica: links to stratosphericozone and atmospheric oxidation capacity, J. Geophys. Res., 110, D23301, doi:10.1029/2005JD006110, 2005.

Gaffney, J. S., Streit, G. E., Spall, W. D., and Hall, J. H.: Beyond acid rain. Do soluble oxidants and organic toxinsinteract with SO_2 and NO_x to increase ecosystem effects?, Environ. Sci. Technol., 21, 519–524, doi:10.1021/es00160a001, 1987.

George, I. J., Matthews, P. S. J., Whalley, L. K., Brooks, B., Goddard, A., Baeza-Romero, M. T., and Heard, D. E.: Measurements of uptake coefficients for heterogeneous loss of HO_2 onto submicron inorganic salt aerosols, Phys. Chem. Chem. Phys., 15, 12829, doi:10.1039/c3cp51831k, 2013.

Guo, S. J., Tan, J. H., Duan, J. C., Ma, Y. L., Yang, F. M., He, K. B., and Hao, J. M.: Characteristics of atmospheric non-methane hydrocarbons during haze episode in Beijing, China, Environ. Monit. Assess., 184, 7235–7246, 2012.

Hall, B. D. and Claiborn, C. S.: Measurements of the dry deposition of peroxides to a Canadian boreal forest, J. Geophys. Res., 102, 29343–29353, doi:10.1029/97JD01113, 1997.

Hall, B. D., Claiborn, C. S., and Baldocchi, D. D.: Measurement and modeling of the dry deposition of peroxides, Atmos. Environ., 33, 577–589, doi:10.1016/s1352-2310(98)00271-4, 1999.

Hammer, M. U., Vogel, B., and Vogel, H.: Findings on H_2O_2/HNO_3 as an indicator of ozone sensitivity in Baden-Wurttemberg, Berlin-Brandenburg, and the Po valley based on numerical simulations, J. Geophys. Res., 107, 8190, doi:10.1029/2000JD000211, 2002.

Hauglustaine, D. A., Granier, C., Brasseur, G. P., and Megie, G.: The importance of atmospheric chemistry in the calcualtion of radiative forcing on the climate system, J. Geophys. Res., 99, 1173–1186, 1994.

He, S. Z., Chen, Z. M., Zhang, X., Zhao, Y., Huang, D. M., Zhao, J. N., Zhu, T., Hu, M., and Zeng, L. M.: Measurement of atmospheric hydrogen peroxide and organic peroxides in Beijing before and during the 2008 Olympic Games: Chemical and phys-

ical factors influencing their concentrations, J. Geophys. Res., 115, D17307, doi:10.1029/2009jd013544, 2010.

Hu, Q. H., Moran, J. E., and Gan, J. Y.: Sorption, degradation, and transport of methyl iodide and other iodine species in geologic media, Appl. Geochem., 27, 774–781, doi:10.1016/j.apgeochem.2011.12.022, 2012.

Hua, W., Chen, Z. M., Jie, C. Y., Kondo, Y., Hofzumahaus, A., Takegawa, N., Chang, C. C., Lu, K. D., Miyazaki, Y., Kita, K., Wang, H. L., Zhang, Y. H., and Hu, M.: Atmospheric hydrogen peroxide and organic hydroperoxides during PRIDE-PRD'06, China: their concentration, formation mechanism and contribution to secondary aerosols, Atmos. Chem. Phys., 8, 6755–6773, doi:10.5194/acp-8-6755-2008, 2008.

Huang, D. M. and Chen, Z. M.: Reinvestigation of the Henry's law constant for hydrogen peroxide with temperature and acidity variation, J. Environ. Sci., 22, 570–574, 2010.

Hyslop, N. P.: Impaired visibility: the air pollution people see, Atmos. Environ., 43, 182–195, doi:10.1016/j.atmosenv.2008.09.067, 2009.

Jacob, D. J.: Heterogeneous chemistry and tropospheric ozone, Atmos. Environ., 34, 2131–2159, doi:10.1016/S1352-2310(99)00462-8, 2000.

Jobson, B. T., Frost, G. J., McKeen, S. A., Ryerson, T. B., Buhr, M. P., Parrish, D. D., Trainer, M., and Fehsenfeld, F. C.: Hydrogen peroxide dry deposition lifetime determined from observed loss rates in a power plant plume, J. Geophys. Res., 103, 22617–22628, doi:10.1029/98JD01619, 1998.

Kim, C. H., Kreidenweis, S. M., Feingold, G., Frost, G. J., and Trainer, M. K.: Modeling cloud effects on hydrogen peroxide and methylhydroperoxide in the marine atmosphere, J. Geophys. Res., 107, D24018, doi:10.1029/2000jd000285, 2002.

Kim, Y. M., Lee, M., Chang, W., Lee, G., Kim, K. R., and Kato, S.: Atmospheric peroxides over the North Pacific during IOC 2002 shipboard experiment, Chemosphere, 69, 1638–1646, doi:10.1016/j.chemosphere.2007.05.057, 2007.

Klippel, T., Fischer, H., Bozem, H., Lawrence, M. G., Butler, T., Jöckel, P., Tost, H., Martinez, M., Harder, H., Regelin, E., Sander, R., Schiller, C. L., Stickler, A., and Lelieveld, J.: Distribution of hydrogen peroxide and formaldehyde over Central Europe during the HOOVER project, Atmos. Chem. Phys., 11, 4391–4410, doi:10.5194/acp-11-4391-2011, 2011.

Kreidenweis, S. M., Petters, M. D., and DeMott, P. J.: Single-parameter estimates of aerosol water content, Environ. Res. Lett., 3, 035002, doi:10.1088/1748-9326/3/3/035002, 2008.

Lang, J., Cheng, S., Wei, W., Zhou, Y., Wei, X., and Chen, D.: A study on the trends of vehicular emissions in the Beijing-Tianjin-Hebei (BTH) region, China, Atmos. Environ., 62, 605–614, doi:10.1016/j.atmosenv.2012.09.006, 2012.

Lee, M., Heikes, B. G., and O'Sullivan, D. W.: Hydrogen peroxide and organic hydroperoxide in the troposphere: a review, Atmos. Environ., 34, 3475–3494, doi:10.1016/s1352-2310(99)00432-x, 2000.

Li, J., Wang, Z., Wang, X., Yamaji, K., Takigawa, M., Kanaya, Y., Pochanart, P., Liu, Y., Irie, H., Hu, B., Tanimoto, H., and Akimoto, H.: Impacts of aerosols on summertime tropospheric photolysis frequencies and photochemistry over Central Eastern China, Atmos. Environ., 45, 1817–1829, doi:10.1016/j.atmosenv.2011.01.016, 2011.

Lin, H. F., Xin, J. Y., Zhang, W. Y., Wang, Y. S., Liu, Z. R., and Chen, C. L.: Comparison of atmospheric particulate matter and aerosol optical depth in Beijing city, Chinese J. of Environ. Sci., 34, 827–834, 2013.

Lind, J. A., Lazrus, A. L., and Kok, G. L.: Aqueous phase oxidation of sulfur (IV) by hydrogen peroxide, methyl hydroperoxide, and peroxyacetic acid, J. Geophys. Res., 92, 4171–4177, 1987.

Liu, Z., Wang, Y., Gu, D., Zhao, C., Huey, L. G., Stickel, R., Liao, J., Shao, M., Zhu, T., Zeng, L., Amoroso, A., Costabile, F., Chang, C.-C., and Liu, S.-C.: Summertime photochemistry during CAREBeijing-2007: RO_x budgets and O_3 formation, Atmos. Chem. Phys., 12, 7737–7752, doi:10.5194/acp-12-7737-2012, 2012.

Loukhovitskaya, E., Bedjanian, Y., Morozov, I., and Le Bras, G.:Laboratory study of the interaction of HO_2 radicals with the NaCl, NaBr, $MgCl_26H_2O$ and sea salt surfaces, Phys. Chem. Chem. Phys., 11, 7896–7905, doi:10.1039/b906300e, 2009.

Ma, X. H., Gan, L., Zhang, A. Y., Li, N. J., and Zhang, M. Y.: Cause analysis on durative fog and haze in January 2013 over Beijing area, Adv. Environ. Protection, 3, 29–33, doi:10.12677/aep.2013.32A006, 2013.

Madronich, S. and Calvert, J. G.: Permutation reactions of organic peroxy-radicals in the troposphere, J. Geophys. Res. 95, 5697–5715, 1990.

Mao, J., Jacob, D. J., Evans, M. J., Olson, J. R., Ren, X., Brune, W. H., Clair, J. M. St., Crounse, J. D., Spencer, K. M., Beaver, M. R., Wennberg, P. O., Cubison, M. J., Jimenez, J. L., Fried, A., Weibring, P., Walega, J. G., Hall, S. R., Weinheimer, A. J., Cohen, R. C., Chen, G., Crawford, J. H., McNaughton, C., Clarke, A. D., Jaeglé, L., Fisher, J. A., Yantosca, R. M., Le Sager, P., and Carouge, C.: Chemistry of hydrogen oxide radicals (HO_x) in the Arctic troposphere in spring, Atmos. Chem. Phys., 10, 5823–5838, doi:10.5194/acp-10-5823-2010, 2010.

Mao, J., Fan, S., Jacob, D. J., and Travis, K. R.: Radical loss in the atmosphere from Cu-Fe redox coupling in aerosols, Atmos. Chem. Phys., 13, 509–519, doi:10.5194/acp-13-509-2013, 2013.

Marcolli, C., Luo, B. P., and Peter, T.: Mixing of the organic aerosol fractions: Liquids as the thermodynamically stable phases, J. Phys. Chem. A, 108, 2216–2224, doi:10.1021/jp036080l, 2004.

Marinoni, A., Parazols, M., Brigante, M., Deguillaume, L., Amato, P., Delort, A.-M., Laj, P., and Mailhot, G.: Hydrogen peroxide in natural cloud water: Sources and photoreactivity, Atmos. Res., 101, 256–263, doi:10.1016/j.atmosres.2011.02.013, 2011.

Martin, R. V.: Global and regional decreases in tropospheric oxidants from photochemical effects of aerosols, J. Geophys. Res., 108, 4097, doi:10.1029/2002jd002622, 2003.

Martin, S. T., Schlenker, J. C., Malinowski, A., Hung, H. M., and Rudich, Y.: Crystallization of atmospheric sulfate-nitrate-ammonium particles, Geophys. Res. Lett., 30, 2102, doi:10.1029/2003gl017930, 2003.

Matthew, B. M., George, I., and Anastasio, C.: Hydroperoxyl radical ($HO_2^{\bullet}$) oxidizes dibromide radical anion ($^{\bullet}Br_2^-$) to bromine (Br_2) in aqueous solution: Implications for the formation of Br_2 in the marine boundary layer, Geophys. Res. Lett., 30, 2297, doi:10.1029/2003gl018572, 2003.

Mogili, P. K., Kleiber, P. D., Young, M. A., and Grassian, V. H.: Heterogeneous uptake of ozone on reactive components of mineral dust aerosol: an environmental aerosol reaction chamber study,

J. Phys. Chem. A, 110, 13799–13807, doi:10.1021/jp063620g, 2006.

Möller, D.: Atmospheric hydrogen peroxide: Evidence for aqueous-phase formation from a historic perspective and a one-year measurement campaign, Atmos. Environ., 43, 5923–5936, doi:10.1016/j.atmosenv.2009.08.013, 2009.

O'Sullivan, D. W., Lee, M., Noone, B. C., and Heikes, B. G.: Henry's law constant determinations for hydrogen peroxide, methyl hydroperoxide,hydroxymethyl hydroperoxide, ethyl hydroperoxide, and peroxyacetic acid, J. Phys. Chem., 100, 3241–3247, 1996.

Penkett, S. A., Jones, B. M. R., Brice, K. A., and Eggleton, A. E. J.: The importance of atmospheric ozone and hydrogen peroxide in oxidising sulphur dioxide in cloud and rainwater, Atmos. Environ., 13, 123–137, 1979.

Phillips, G. J., Pouvesle, N., Thieser, J., Schuster, G., Axinte, R., Fischer, H., Williams, J., Lelieveld, J., and Crowley, J. N.: Peroxyacetyl nitrate (PAN) and peroxyacetic acid (PAA) measurements by iodide chemical ionisation mass spectrometry: first analysis of results in the boreal forest and implications for the measurement of PAN fluxes, Atmos. Chem. Phys., 13, 1129–1139, doi:10.5194/acp-13-1129-2013, 2013.

Pradhan, M., Kalberer, M., Griffiths, P. T., Braban, C. F., Pope, F. D., Cox, R. A., and Lambert, R. M.: Uptake of gaseous hydrogen peroxide by submicrometer titanium dioxide aerosol as a function of relative humidity, Environ. Sci. Technol., 44, 1360–1365, doi:10.1021/es902916f, 2010a.

Pradhan, M., Kyriakou, G., Archibald, A. T., Papageorgiou, A. C., Kalberer, M., and Lambert, R. M.: Heterogeneous uptake of gaseous hydrogen peroxide by Gobi and Saharan dust aerosols: a potential missing sink for H_2O_2 in the troposphere, Atmos. Chem. Phys., 10, 7127–7136, doi:10.5194/acp-10-7127-2010, 2010b.

Prather, M. J., Holmes, C. D., and Hsu, J.: Reactive greenhouse gas scenarios: Systematic exploration of uncertainties and the role of atmospheric chemistry, Geophys. Res. Lett., 39, L09803, doi:10.1029/2012gl051440, 2012.

Ran, L., Zhao, C. S., Xu, W. Y., Han, M., Lu, X. Q., Han, S. Q., Lin, W. L., Xu, X. B., Gao, W., Yu, Q., Geng, F. H., Ma, N., Deng, Z. Z., and Chen, J.: Ozone production in summer in the megacities of Tianjin and Shanghai, China: a comparative study, Atmos. Chem. Phys., 12, 7531–7542, doi:10.5194/acp-12-7531-2012, 2012.

Reeves, C. E. and Penkett, S. A.: Measurements of peroxides and what they tell us, Chem. Rev., 103, 5199–5218, doi:10.1021/cr0205053, 2003.

Sander, S. P., Abbatt, J., Barker, J. R., Burkholder, J. B., Friedl, R. R., Golden, D. M., Huie, R. E., Kolb, C. E., Kurylo, M. J., Moortgat, G. K., Orkin, V. L., and Wine, P. H.: Chemical Kinetics and Photochemical Data for Use in Atmospheric Studies, Evaluation No. 17, JPL Publication 10-6, Jet Propulsion Laboratory, Pasadena, CA, USA, available at:http://jpldataeval.jpl.nasa.gov (last access: June 2012), 2011.

Sauer, F., Schuster, G., Schäfer, C., and Moortgat, G. K.: Determination of H_2O_2 and organic peroxides in cloud- and rain-water on the Kleiner Feldberg during FELDEX, Geophys. Res. Lett., 23, 2605–2608, 1996.

Sauer, F., Beck, J., Schustera, G., and Moortgat, G. K.: Hydrogen peroxide, organic peroxides and organic acids in a forested area during FIELDVOC'94, Chemosphere, Global Change Sci., 3, 309–326, 2001.

Schaap, M., Apituley, A., Timmermans, R. M. A., Koelemeijer, R. B. A., and de Leeuw, G.: Exploring the relation between aerosol optical depth and $PM_{2.5}$ at Cabauw, the Netherlands, Atmos. Chem. Phys., 9, 909–925, doi:10.5194/acp-9-909-2009, 2009.

Schuchmann, M. N. and von Sonntag, C.: The rapid hydration of the acetyl radical. A pulse-radiolysis study of acetaldehyde in aqueous-solution, J. Am. Chem. Soc., 110, 5698–5701, doi:10.1021/ja00225a019, 1988.

Schwartz, S. E.: Mass-transport considerations pertinent to aqueous phase reactions of gases in liquid-water clouds, Chem. Multiphase Atmos. Syst., 6, 415–471, 1986.

Shen, H., Barakat, A. I., and Anastasio, C.: Generation of hydrogen peroxide from San Joaquin Valley particles in a cell-free solution, Atmos. Chem. Phys., 11, 753–765, doi:10.5194/acp-11-753-2011, 2011.

Stein, A. F. and Saylor, R. D.: Sensitivities of sulfate aerosol formation and oxidation pathways on the chemical mechanism employed in simulations, Atmos. Chem. Phys., 12, 8567–8574, doi:10.5194/acp-12-8567-2012, 2012.

Stickler, A., Fischer, H., Bozem, H., Gurk, C., Schiller, C., Martinez-Harder, M., Kubistin, D., Harder, H., Williams, J., Eerdekens, G., Yassaa, N., Ganzeveld, L., Sander, R., and Lelieveld, J.: Chemistry, transport and dry deposition of trace gases in the boundary layer over the tropical Atlantic Ocean and the Guyanas during the GABRIEL field campaign, Atmos. Chem. Phys., 7, 3933–3956, doi:10.5194/acp-7-3933-2007, 2007.

Sun, Y., Zhuang, G., Wang, Y., Han, L., Guo, J., Dan, M., Zhang, W., Wang, Z., and Hao, Z.: The air-borne particulate pollution in Beijing? concentration, composition, distribution and sources, Atmos. Environ., 38, 5991–6004, doi:10.1016/j.atmosenv.2004.07.009, 2004.

Sun, Y., Zhuang, G., Tang, A., Wang, Y., and An, Z.: Chemical characteristics of $PM_{2.5}$ and PM_{10} in haze-fog episodes in Beijing, Environ. Sci. Technol., 40, 3148–3155, doi:10.1021/es051533g, 2006.

Sun, Y., Wang, Z., Dong, H., Yang, T., Li, J., Pan, X., Chen, P., and Jayne, J. T.: Characterization of summer organic and inorganic aerosols in Beijing, China with an Aerosol Chemical Speciation Monitor, Atmos. Environ., 51, 250–259, doi:10.1016/j.atmosenv.2012.01.013, 2012.

Taketani, F., Kanaya, Y., and Akimoto, H.: Kinetics of heterogeneous reactions of HO_2 radical at ambient concentration levels with $(NH_4)_2SO_4$ and NaCl aerosol Particles, J. Phys. Chem. A., 112, 2370–2377, 2008.

Taketani, F., Kanaya, Y., and Akimoto, H.: Heterogeneous loss of HO_2 by KCl, synthetic sea salt, and natural seawater aerosol particles, Atmos. Environ., 43, 1660–1665, 2009.

Taketani, F., Kanaya, Y., and Akimoto, H.: Kinetics of HO_2 uptake in levoglucosan and polystyrene latex particles, J. Phys. Chem. Lett., 1, 1701–1704, doi:10.1021/jz100478s, 2010.

Taketani, F., Kanaya, Y., Pochanart, P., Liu, Y., Li, J., Okuzawa, K., Kawamura, K., Wang, Z., and Akimoto, H.: Measurement of overall uptake coefficients for HO_2 radicals by aerosol particles sampled from ambient air at Mts. Tai and Mang (China), Atmos. Chem. Phys., 12, 11907–11916, doi:10.5194/acp-12-11907-2012, 2012.

Thornton, J. and Abbatt, J. P. D.: Measurements of HO_2 uptake to aqueous aerosol: Mass accommodation coefficients and net reactive loss, J. Geophys. Res., 110, D08309, doi:10.1029/2004jd005402, 2005.

Valverde-Canossa, J., Ganzeveld, L., Rappenglück, B., Steinbrecher, R., Klemm, O., Schuster, G., and Moortgat, G. K.: First measurements of H_2O_2 and organic peroxides surface fluxes by the relaxed eddy-accumulation technique, Atmos. Environ., 40, S55–S67, doi:10.1016/j.atmosenv.2006.03.038, 2006.

Walker, S. J., Evans, M. J., Jackson, A. V., Steinbacher, M., Zellweger, C., and McQuaid, J. B.: Processes controlling the concentration of hydroperoxides at Jungfraujoch Observatory, Switzerland, Atmos. Chem. Phys., 6, 5525–5536, doi:10.5194/acp-6-5525-2006, 2006.

Wang, B., Shao, M., Lu, S. H., Yuan, B., Zhao, Y., Wang, M., Zhang, S. Q., and Wu, D.: Variation of ambient non-methane hydrocarbons in Beijing city in summer 2008, Atmos. Chem. Phys., 10, 5911–5923, doi:10.5194/acp-10-5911-2010, 2010.

Wang, Y., Zhuang, G. S., Tang, A. H., Yuan, H., Sun, Y. L., Chen, S. A., and Zheng, A. H.: The ion chemistry and the source of $PM_{2.5}$ aerosol in Beijing, Atmos. Environ., 39, 3771–3784, doi:10.1016/j.atmosenv.2005.03.013, 2005.

Wang, Y., Zhuang, G. S., Sun, Y. L., and An, Z. S.: The variation of characteristics and formation mechanisms of aerosols in dust, haze, and clear days in Beijing, Atmos. Environ., 40, 6579–6591, 2006.

Wang, Y., Arellanes, C., Curtis, D. B., and Paulson, S. E.: Probing the source of hydrogen peroxide associated with coarse mode aerosol particles in southern California, Environ. Sci. Technol., 44, 4070–4075, doi:10.1021/es100593k, 2010.

Wang, Y., Kim, H., and Paulson, S. E.: Hydrogen peroxide generation from α- and β-pinene and toluene secondary organic aerosols, Atmos. Environ., 45, 3149–3156, doi:10.1016/j.atmosenv.2011.02.060, 2011.

Wang, Y., Arellanes, C., and Paulson, S. E.: Hydrogen peroxide associated with ambient fine-mode, diesel, and biodiesel aerosol particles in Southern California, Aerosol Sci. Tech., 46, 394–402, doi:10.1080/02786826.2011.633582, 2012.

Wang, Y. H., Ridley, B., Fried, A., Cantrell, C., Davis, D., Chen, G., Snow, J., Heikes, B., Talbot, R., Dibb, J., Flocke, F., Weinheimer, A., Blake, N., Blake, D., Shetter, R., Lefer, B., Atlas, E., Coffey, M., Walega, J., and Wert, B.: Springtime photochemistry at northern mid and high latitudes, J. Geophys. Res., 108, 8358, doi:10.1029/2002jd002227, 2003.

Weller, R., Schrems, O., Boddenberg, A., Gab, S., and Gautrois, M.: Meridional distribution of hydroperoxides and formaldehyde in the marine boundary layer of the Atlantic (48° N– 35° S) measured during the Albatross campaign, J. Geophys. Res., 105, 14401–14412, 2000.

Willey, J. D., Glinski, D. A., Southwell, M., Long, M. S., Brooks Avery Jr., G., and Kieber, R. J.: Decadal variations of rainwater formic and acetic acid concentrations in Wilmington, NC, USA, Atmos. Environ., 45, 1010–1014, doi:10.1016/j.atmosenv.2010.10.047, 2011.

Xia, X. A., Chen, H. B., Wang, P. C., Zhang, W. X., Goloub, P., Chatenet, B., Eck, T. F., and Holben, B. N.: Variation of column-integrated aerosol properties in a Chinese urban region, J. Geophys. Res., 111, D05204, doi:10.1029/2005jd006203, 2006.

Xu, Z. and Han, G.: Chemical and strontium isotope characterization of rainwater in Beijing, China, Atmos. Environ., 43, 1954–1961, doi:10.1016/j.atmosenv.2009.01.010, 2009.

Xu, Z., Tang, Y., and Ji, J.: Chemical and strontium isotope characterization of rainwater in Beijing during the 2008 Olympic year, Atmos. Res., 107, 115–125, doi:10.1016/j.atmosres.2012.01.002, 2012.

Yadav, A. K., Kumar, K., Kasim, A. M. B. H. A., Singh, M. P., Parida, S. K., and Sharan, M.: Visibility and incidence of respiratory diseases during the 1998 haze episode in Brunei Darussalam, Pure Appl. Geophys., 160, 265–277, 2003.

Yu, X. N., Zhu, B., Yin, Y., Yang, J., Li, Y. W., and Bu, X. L.: A comparative analysis of aerosol properties in dust and haze-fog days in a Chinese urban region, Atmos. Res., 99, 241–247, 2011.

Yue, D. L., Hu, M., Wu, Z. J., Wang, Z. B., Guo, S., Wehner, B., Nowak, A., Achtert, P., Wiedensohler, A., Jung, J., Kim, Y. J., and Liu, S. C.: Characteristics of aerosol size distributions and new particle formation in the summer in Beijing, J. Geophys. Res., 114, D00G12, doi:10.1029/2008jd010894, 2009.

Zhang, L., Moran, M. D., Makar, P. A., Brook, J. R., and Gong, S.: Modelling gaseous dry deposition in AURAMS: a unified regional air-quality modelling system, Atmos. Environ., 36, 537–560, doi:10.1016/S1352-2310(01)00447-2, 2002.

Zhang, X., Chen, Z. M., He, S. Z., Hua, W., Zhao, Y., and Li, J. L.: Peroxyacetic acid in urban and rural atmosphere: concentration, feedback on PAN-NO_x cycle and implication on radical chemistry, Atmos. Chem. Phys., 10, 737–748, doi:10.5194/acp-10-737-2010, 2010.

Zhang, X., He, S. Z., Chen, Z. M., Zhao, Y., and Hua, W.: Methyl hydroperoxide (CH_3OOH) in urban, suburban and rural atmosphere: ambient concentration, budget, and contribution to the atmospheric oxidizing capacity, Atmos. Chem. Phys., 12, 8951–8962, doi:10.5194/acp-12-8951-2012, 2012.

Zhang, Y. J., Mu, Y. J., Liu, J. F., and Mellouki, A.: Levels, sources and health risks of carbonyls and BTEX in the ambient air of Beijing, China, J. Environ. Sci., 24, 124–130, doi:10.1016/s1001-0742(11)60735-3, 2012.

Zhao, Y., Chen, Z. M., Shen, X. L., and Zhang, X.: Kinetics and mechanisms of heterogeneous reaction of gaseous hydrogen peroxide on mineral oxide particles, Environ. Sci. Technol., 45, 3317–3324, doi:10.1021/es104107c, 2011.

Zhao, Y., Chen, Z. M., Shen, X. L., and Huang, D.: Heterogeneous reactions of gaseous hydrogen peroxide on pristine and acidic gas-processed calcium carbonate particles: Effects of relative humidity and surface coverage of coating, Atmos. Environ., 67, 63–72, doi:10.1016/j.atmosenv.2012.10.055, 2013.